A Search for a keV Signature of Radiatively Decaying Dark Matter with *Suzaku XIS* and Future Missions

N. Y. Yamasaki with much help by
N. Sekiya, K. Mitsuda, R. Yamamoto
(ISAS/JAXA)

Outline

1. Introduction: Why astrophysical search in keV range ?
2. Strategy of our study
   - Selection of targets and detectors
3. Analysis details: We need to be very careful !
   - Line search and LEE effect
4. Future prospects and Conclusion

Introduction

DM candidates

Table 1 Summary of dark matter particle candidates, their properties, and their potential methods of detection

	WIMPs	SuperWIMPs	Light $\tilde{G}$	Hidden DM	Sterile ν	Axions
Motivation	GHP	GHP	GHP/NPFP	GHP/NPFP	ν Mass	Strong CP
Naturally Correct Ω	Yes	Yes	No	Possible	No	No
Production Mechanism	Freeze Out	Decay	Thermal	Various	Various	Various
Mass Range	GeV-TeV	GeV-TeV	eV-keV	GeV−TeV	keV	μeV−meV
Temperature	Cold	Cold/Warm	Cold/Warm	Cold/Warm	Warm	Cold
Collisional				√		
Early Universe		√√		√		
Direct Detection	√√			√		√√
Indirect Detection	√√	√		√	√√	
Particle Colliders	√√	√√	√√	√		

The particle physics motivations are discussed in Section 2.2; GHP and NPFP are abbreviations for the gauge hierarchy problem and new physics flavor problem, respectively. In the last five rows, √√ denotes detection signals that are generic for this class of dark matter candidate and √ denotes signals that are possible, but not generic. "Early Universe" includes phenomena such as BBN (Big Bang nucleosynthesis) and the CMB (cosmic microwave background); "Direct Detection" implies signatures from dark matter scattering off normal matter in the laboratory; "Indirect Detection" implies signatures of late time dark matter annihilation or decay; and "Particle Colliders" implies signatures of dark matter or its progenitors produced at colliders, such as the Large Hadron Collider (LHC). See the text for details.

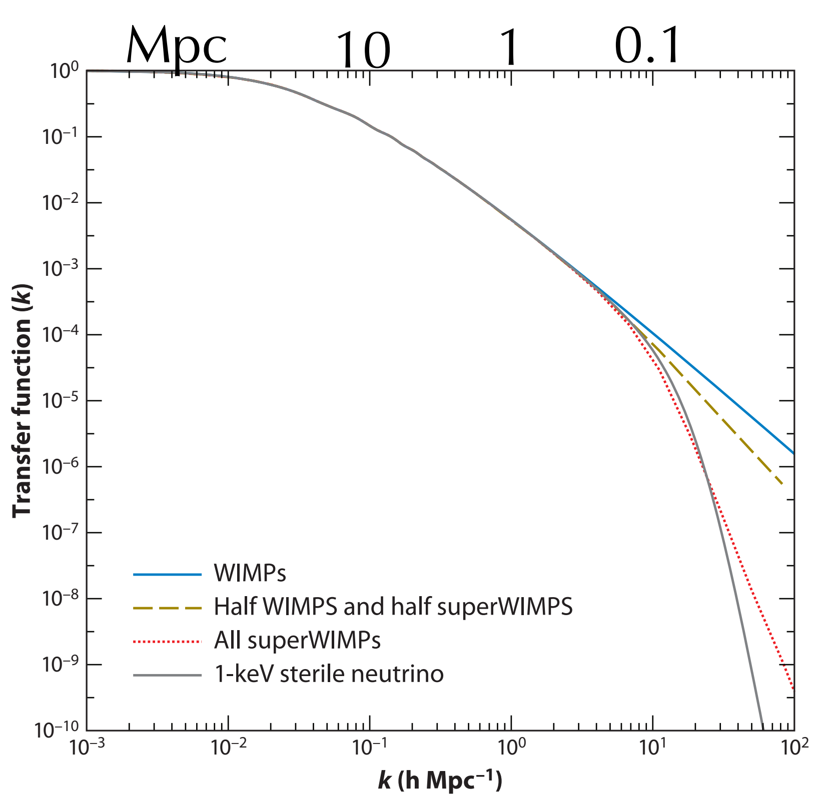

Feng , 2010

Sterile ν (4th right-handed ν) in keV can suppress the small scale fluctuation, and solve "sub-halo" problem.

Expected intensity by astrophysical observation

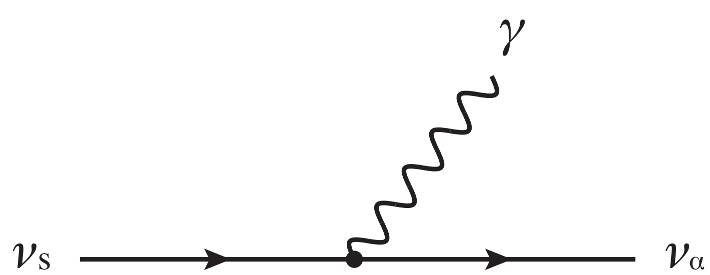

$$\Gamma = \frac{9\alpha {G_F}^2}{1024\pi^2} {m_s}^5 \sin^2 2\theta$$
$$= 1.4 \times 10^{-32} \left(\frac{m_s}{1\ \mathrm{keV}}\right)^5 \left(\frac{\sin^2 2\theta}{10^{-10}}\right)\ \mathrm{s}^{-1},$$

$$I = \frac{\Gamma S_{DM}}{4\pi m_{DM}},\ S_{DM} = \int_{l.o.s.} \rho_{DM}(r) dr$$

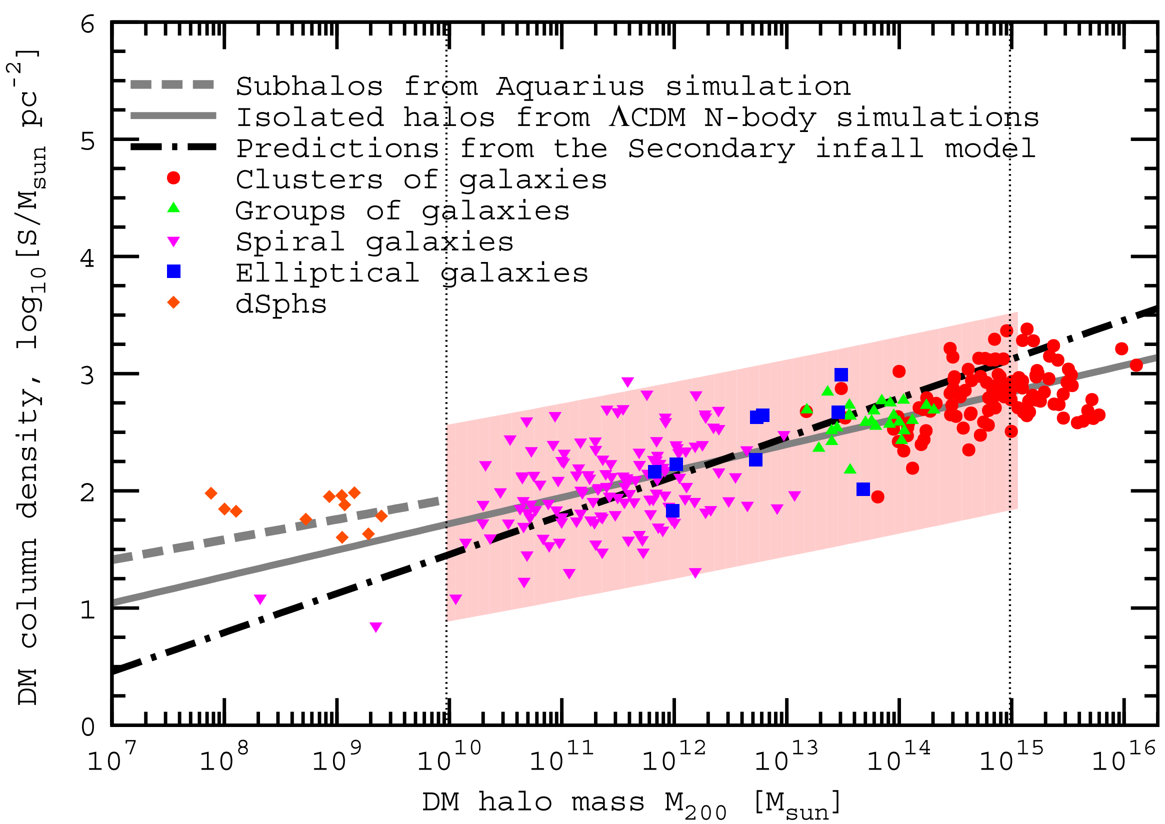

"Column density" in the fov S_{DM} is proportional to the signal ⇒ (Milky Way and extra) galaxies

& clusters of galaxies can be good targets.

Boyarsky et al. 2010

Many studies

Table 2.1 Previous searches for a keV signature of dark matter (examples).

Reference	Target	Instrument (Satellite)	Exposure [ksec]	Note
Boyarsky+ 2006b	MW*	XMM-Newton	1450	
Boyarsky+ 2006c	Coma, Virgo	XMM-Newton	20, 40	
Boyarsky+ 2006d	LMC†	XMM-Newton	20	
Riemer-Sørensen+ 2006	MW	Chandra	–	
Watson+ 2006	M31 center	XMM-Newton	35	
Riemer-Sørensen+ 2007	A520	Chandra	67	
Boyarsky+ 2007	MW, UMi‡	XMM-Newton	547, 7	
Abazajian+ 2007	MW	Chandra	1500	
Boyarsky+ 2008	Bullet Cluster	Chandra	450	
Boyarsky+ 2009	M31 center	XMM-Newton	130	
Loewenstein+ 2009	UMi‡	Suzaku	70	
Riemer-Sørensen+ 2009	Draco§	Chandra	32	
Loewenstein+ 2010	Willman 1§	Chandra	100	2.5 keV line (1.8σ).
Prokhonov+ 2010	MW center	Suzaku	370	8.7 keV line (3.0σ).
Boyarsky+ 2010	M31, Fornax, Sculptor	XMM-Newton, Chandra	400, 52, 162	No 2.5 keV line.
Nieto+ 2010	Willman 1§	Chandra	100	No 2.5 keV line.
Borriello+ 2012	M33	XMM-Newton	20 – 30	
Watson+ 2012	M31 off-center	Chandra	53	
Loewenstein+ 2012	Willman 1	XMM-Newton	60	
Kusenko+ 2013	UMi, Draco	Suzaku	200, 200	
Horiuchi+ 2014	M31	Chandra	404	
Bulbul+ 2014	Clusters	XMM-Newton	8855	3.5 keV line (4.3σ).
Boyarsky+ 2014a	M31, Perseus	XMM-Newton	2452, 745	3.5 keV line (4.4σ).
	MW	XMM-Newton	15700	No 3.5 keV line.
Boyarsky+ 2014b	MW center	XMM-Newton	2640	3.5 keV line (5.7σ).

Notes.
∗ The Milky Way galaxy.
† Large Magellanic Cloud.
‡ UMi: Ursa Minor dwarf galaxy.
§ Dwarf galaxies (satellite galaxies of the Milky Way)

Table 2.2 Detection reports of the possible 3.5 keV signature (Iakubovskyi, 2014).

Reference	Target	Instrument	Exposure [ksec]	Energy [keV]	Intensity [10^{-6} cm^{-2} s^{-1}]
Bulbul+ 2014	Full stacked clusters	MOS†	6784	3.57±0.02	4.0±0.8
	Full stacked clusters	PN†	2071	3.51±0.03	$3.9^{+0.6}_{-1.0}$
	Coma+Cen+Oph*	MOS	525	3.57(fix)	$15.9^{+3.4}_{-3.8}$
	Coma+Cen+Oph	PN	184	3.57(fix)	< 9.5(90%)
	Perseus*	MOS	317	3.57(fix)	$52.0^{+24.1}_{-15.2}$
	Perseus	PN	38	3.57(fix)	< 17.7(90%)
	Perseus	MOS	317	3.57(fix)	$21.4^{+7.0}_{-6.3}$
	Perseus	PN	38	3.57(fix)	< 16.1(90%)
	Clusters	MOS	5941	3.57(fix)	$2.1^{+0.4}_{-0.5}$
	Clusters	PN	1849	3.57(fix)	$2.0^{+0.3}_{-0.5}$
	Perseus	ACIS-S‡	0.9	3.56±0.02	$10.2^{+3.7}_{-3.5}$
	Perseus	ACIS-I‡	0.5	3.56(fix)	$18.6^{+7.8}_{-8.0}$
	Virgo*	ACIS-I	0.5	3.56(fix)	< 9.1(90%)
Boyarsky+ 2014a	M31	MOS	979	3.53±0.03	$4.9^{+1.6}_{-1.3}$
	M31	MOS	1473	3.50 – 3.56	< 1.8(2σ)
	Perseus	MOS	529	3.50±0.04	7.0±2.6
	Perseus	PN	216	3.46±0.04	9.2±3.1
	MW	MOS	15700	3.45 – 3.58	< 0.7(2σ)
Riemer-Sørensen+ 2014	MW center	ACIS-I	751	∼3.5	< 25(2σ)
Jeltema+ 2014	MW center	MOS	1375	∼3.5	< 41
	MW center	PN	487	∼3.5	< 32
	M31	MOS	979	3.53±0.07	2.1±1.5
Boyarsky+ 2014b	MW center	MOS	2640	3.539±0.011	29±5
Malyshev+ 2014	Combined dSphs	MOS+PN	822+233	3.55(fix)	< 0.254(90%)
Urban+ 2014	Perseus core	XIS§	740	$3.510^{+0.023}_{-0.008}$	$32.5^{+3.7}_{-4.3}$
	Perseus confined	XIS	740	$3.592^{+0.021}_{-0.024}$	$18.8^{+6.5}_{-5.5}$
	Coma*	XIS	164	∼3.45	∼30
	Ophiuchus*	XIS	83	∼3.45	∼40
	Virgo	XIS	90	3.55	< 6.5(2σ)

Notes.
∗ Clusters of galaxies.
† X-ray CCD instruments of XMM-Newton.
‡ X-ray CCD instruments of Chandra.
§ X-ray CCD instruments of Suzaku.

Summarized by Sekiya PhD thesis (2015)

3.5 keV line ?

(3.55-3.57)±0.03 keV line from clusters of galaxies (Bulbul+2014)

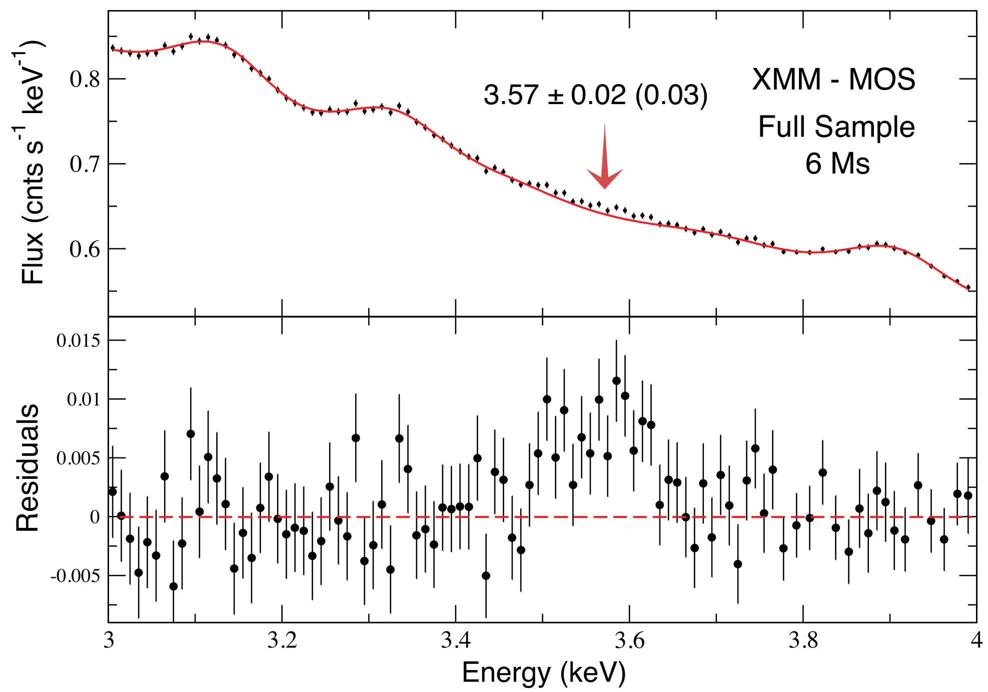

Figure 6. 3–4 keV band of the stacked *XMM-Newton* MOS spectrum of the full sample. The spectrum was rebinned to make the excess at ~3.57 keV more apparent.

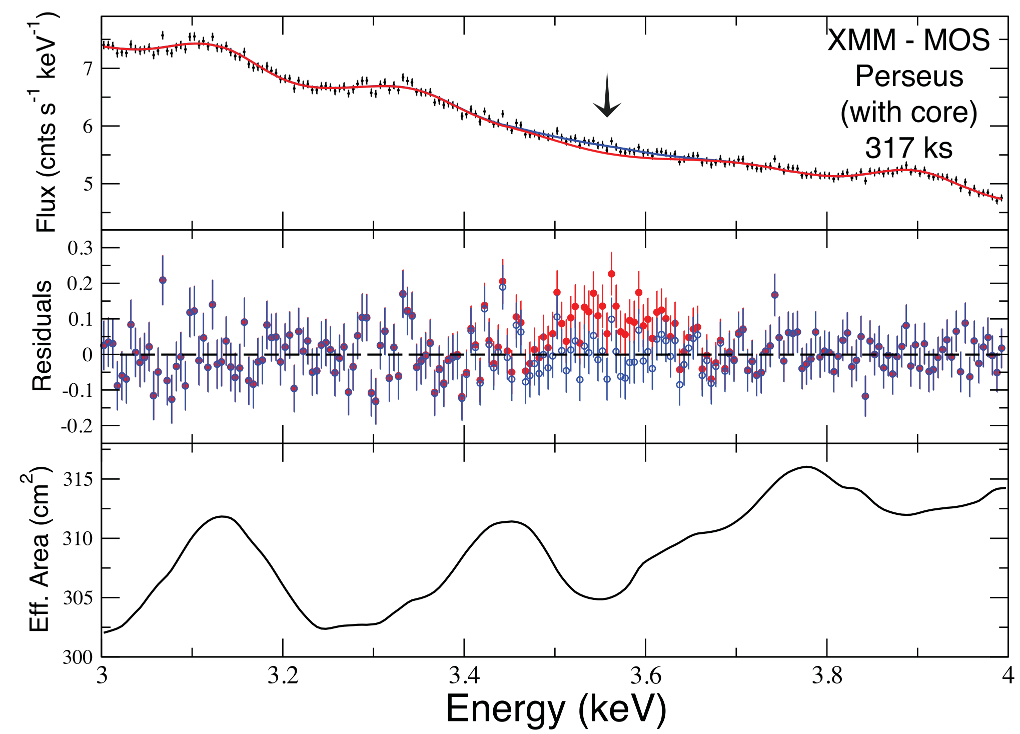

No detection in M31 and GC (Jeltema & Profumo 2015)

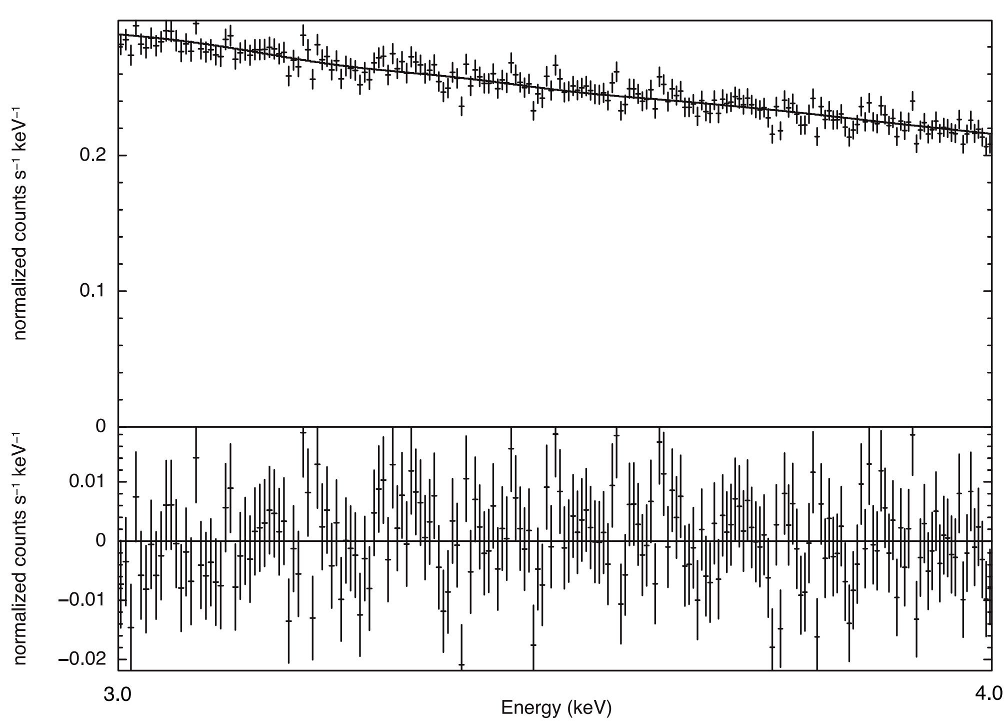

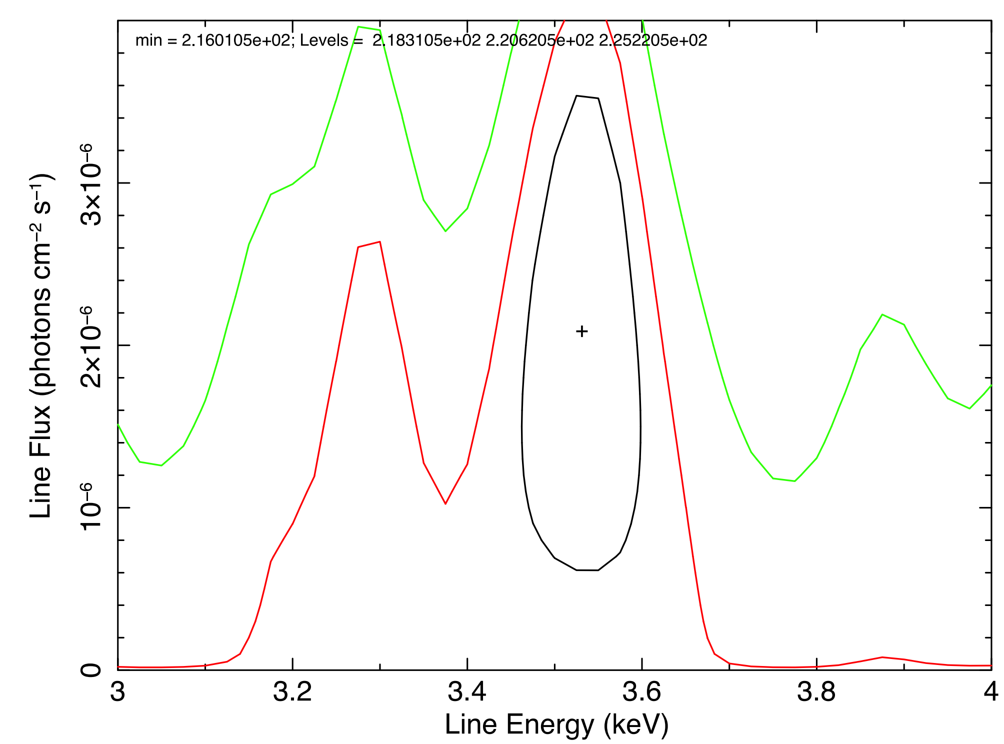

Suzaku search for DM in Perseus cluster

Suzaku is also sensitive to detect Cr lines

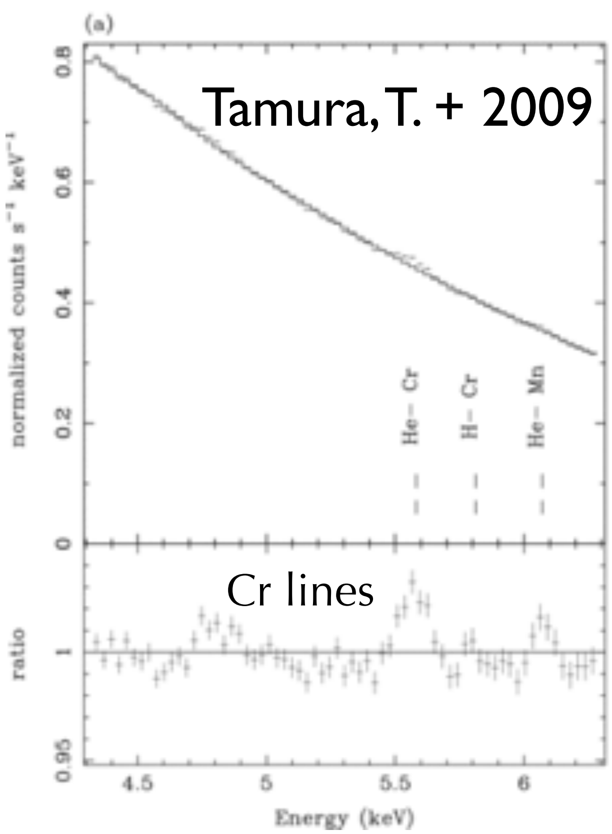

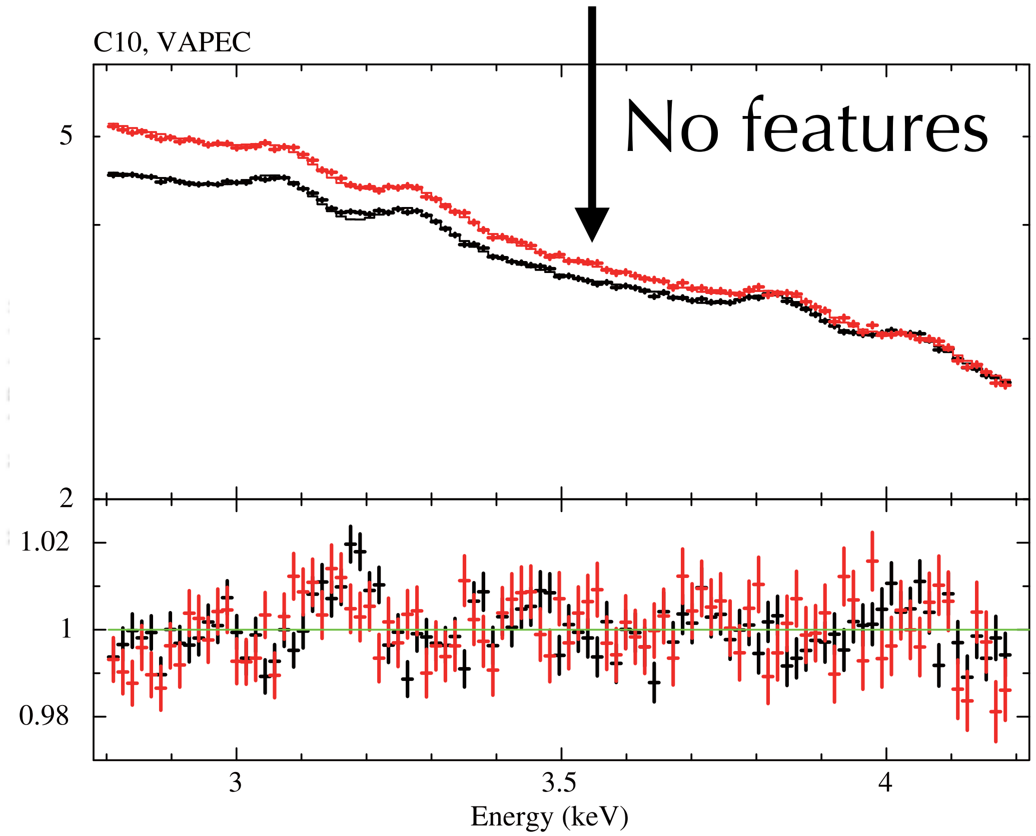

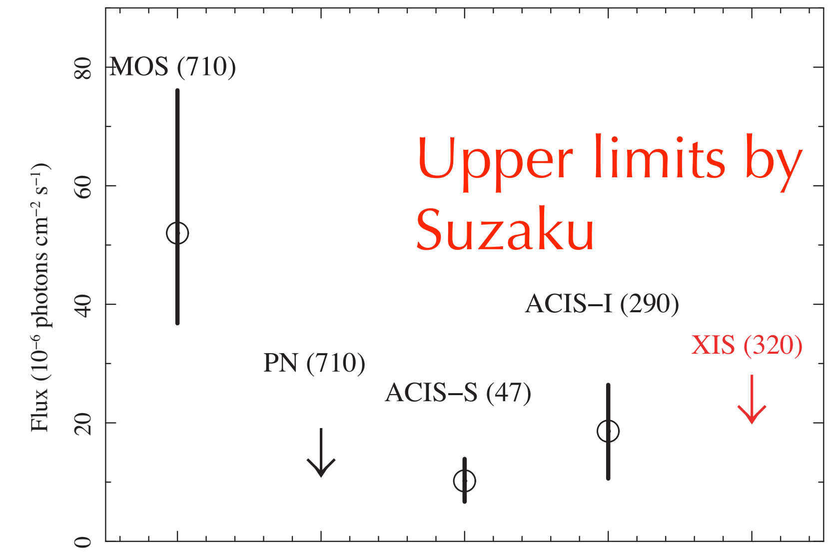

Table 4. Suzaku XIS and XMM-Newton EPIC observations.

Detector	Area* (cm^2)	FOV† ($arcmin^2$)	exp‡ (ks)	Area × exp (10^6 cm^2 s)	Area× exp × FOV (10^9 cm^2 s $arcmin^2$)
XIS/FI	260	320	1040	270	86.5
XIS/BI	260	320	530	138	44.1
Total	—	—	—	408	130.6
MOS	300	710	317	95.1	67.5
pn	700	710	38	26.6	18.9

*Effective area at energy of 3.5 keV.
†Detector's field of view.
‡Exposure time. EPIC values are those of Bulbul et al. (2014). The FI and MOS exposures are the sums of those of each sensor (i.e., XIS-0+XIS-3 or MOS-1+MOS-2).

Tamura, T. +, 2015, PASJ, 67,23

X-ray view of Perseus Cluster

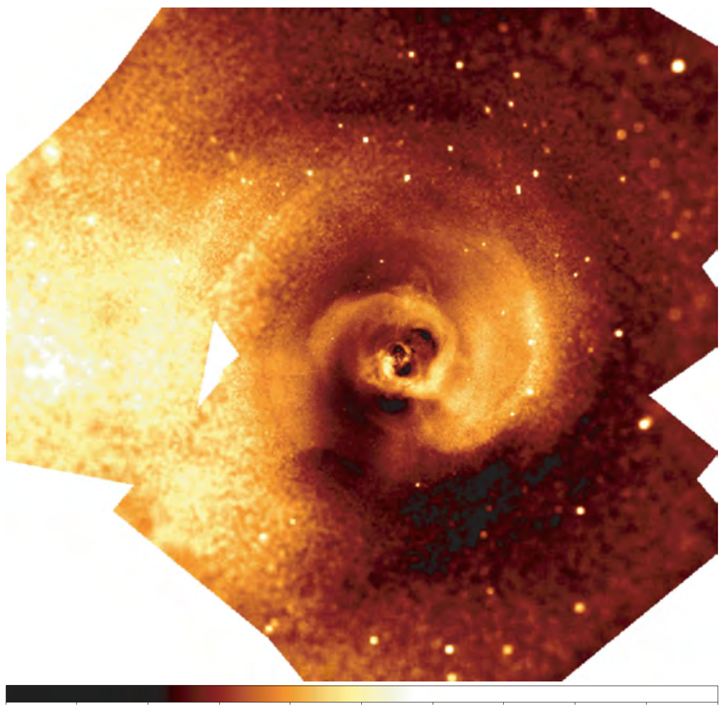

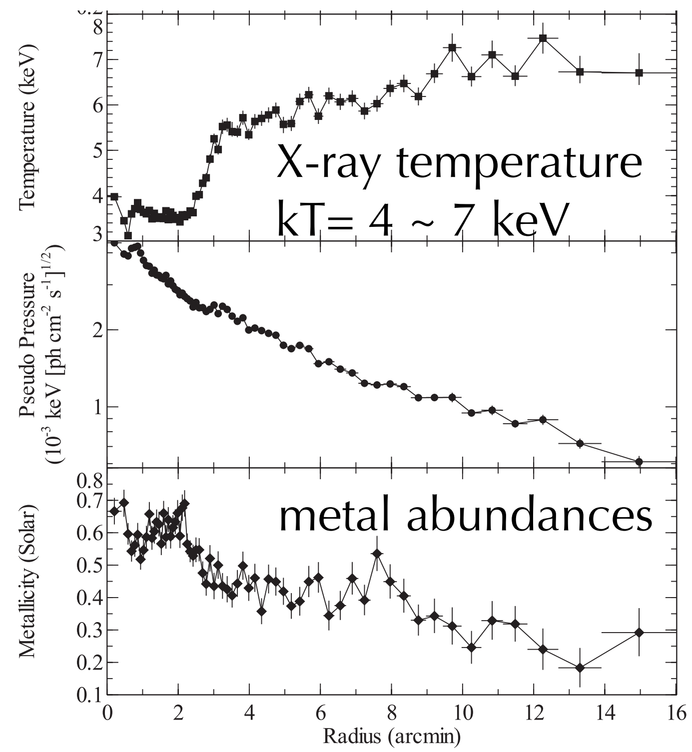

Center of the Perseus cluster is very complicated.
The X-ray emission is very bright with many emission lines, and the temperature and abundance is not uniform.

Fabian + 2011

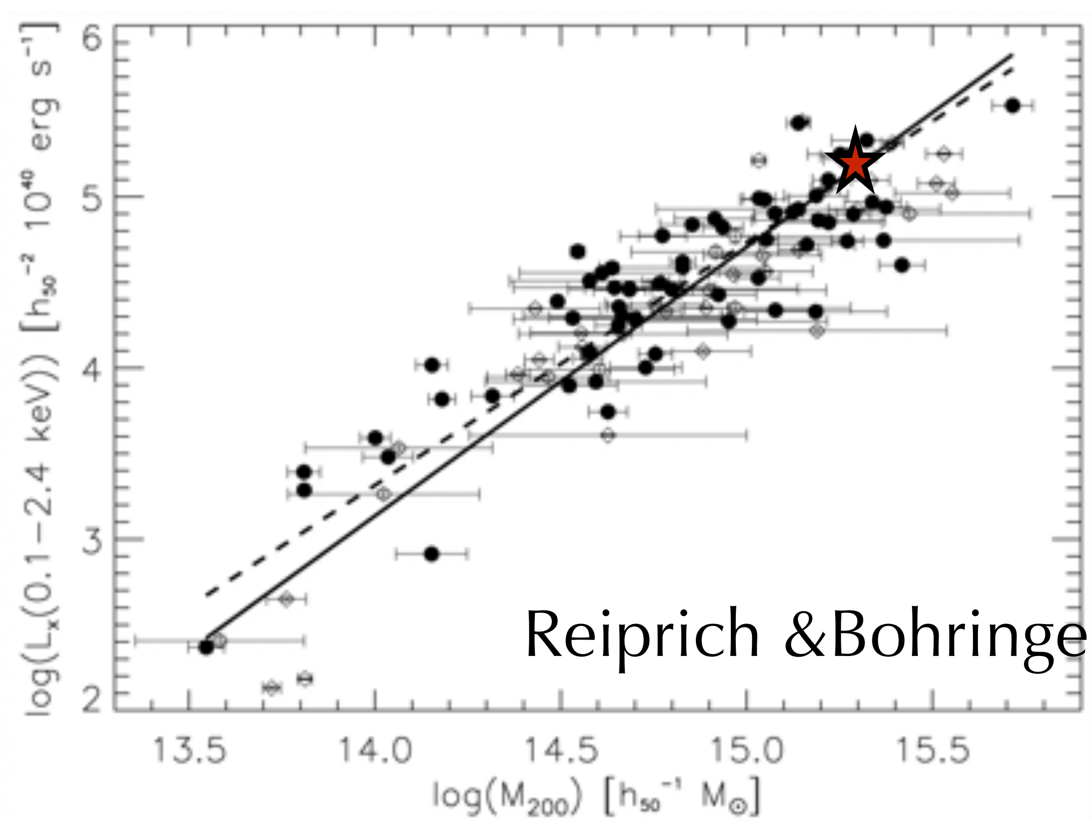

Reiprich &Bohringer 2002

Heavy system has lots of DM and baryons.

$$\log\left[\frac{L_X(0.1\text{–}2.4\ \text{keV})}{h_{50}^{-2}\,10^{40}\ \text{ergs s}^{-1}}\right] = A + \alpha \log\left(\frac{M_{200}}{h_{50}^{-1}\,M_\odot}\right)$$

$\alpha \sim 1.6$

X-ray emission spectrum from hot plasma

Continuum (Bremstrahlung by electrons) + many emission lines
Emission line pattern changes by temperature and metal abundances.

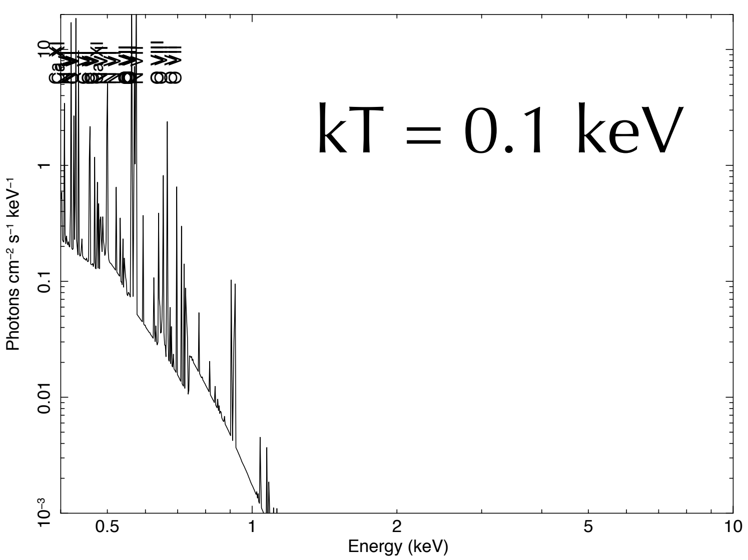

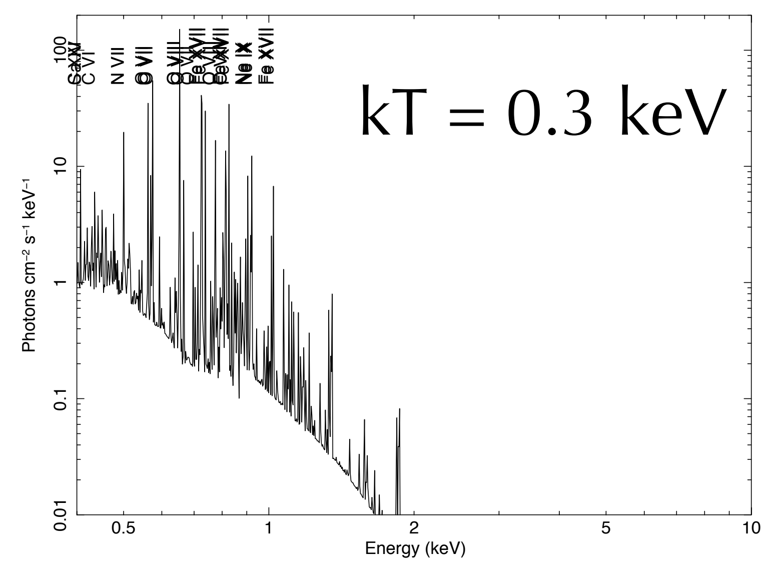

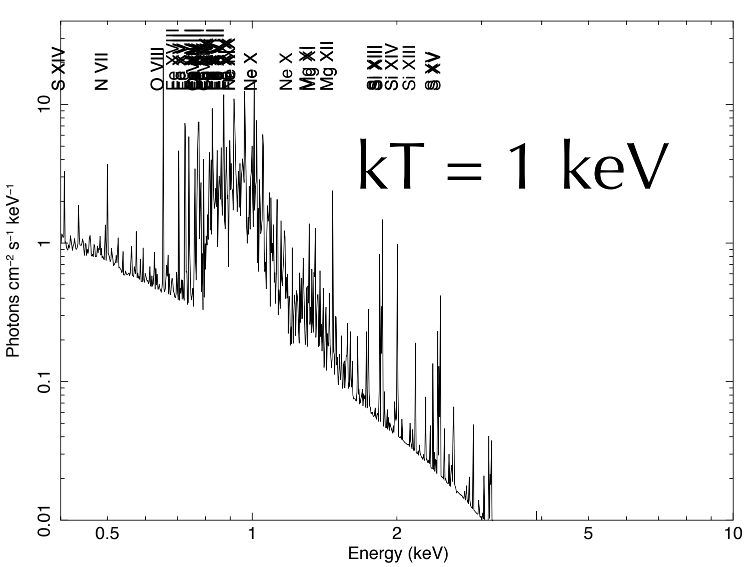

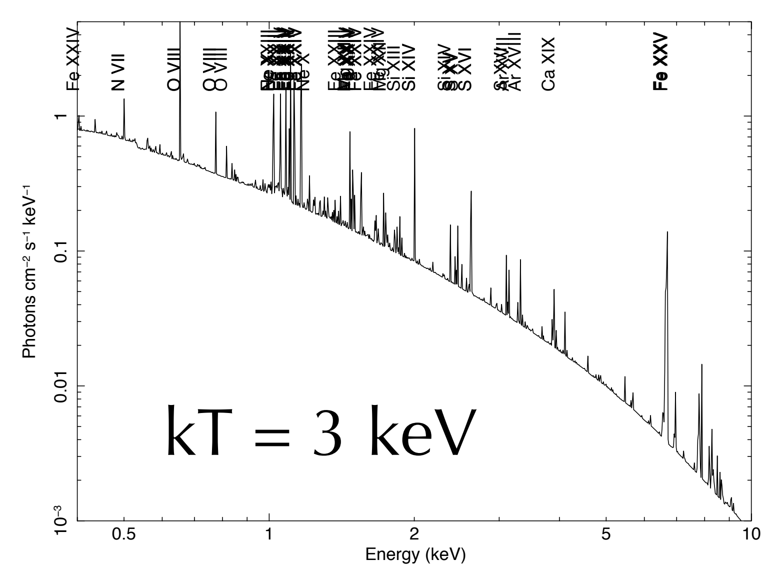

X-ray view of M31

(NASA/ Z Li & Q.D.Wang)

28 arcminutes

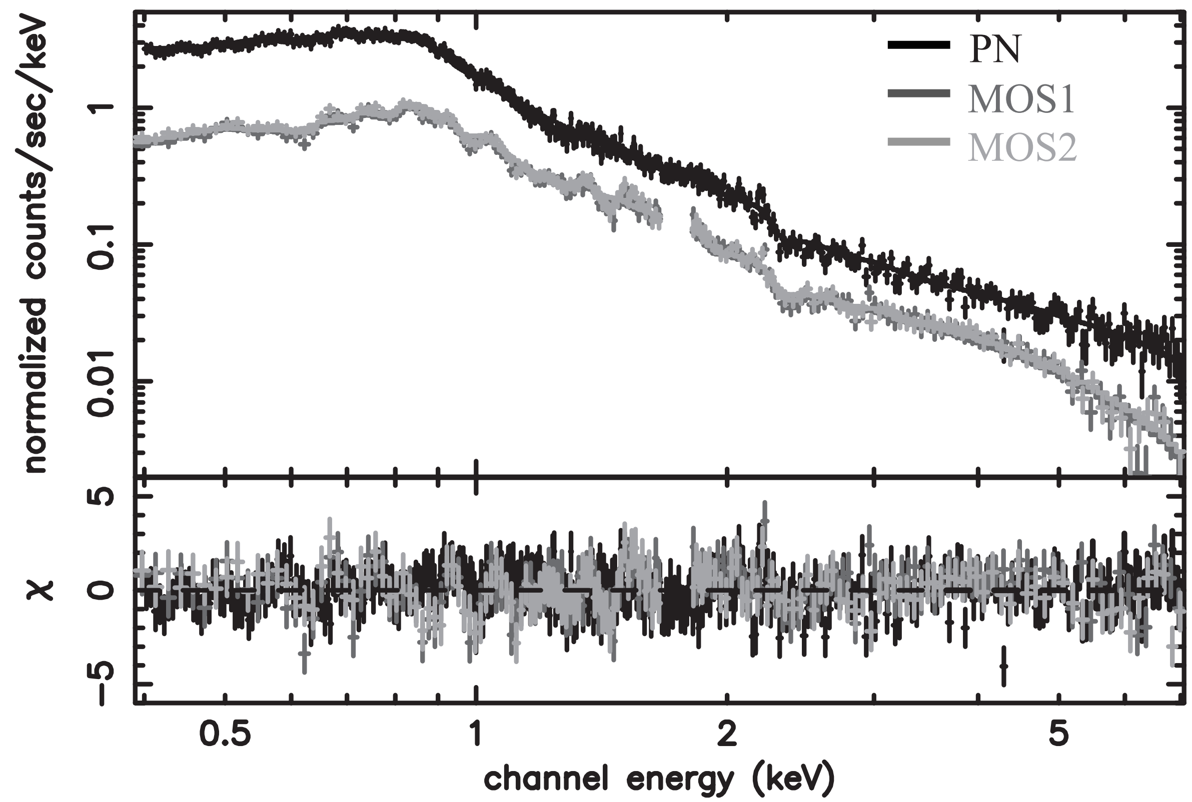

FIG. 5.—Same as Fig. 4 but with the fit performed over the full 0.4–7 keV energy range using the LMXB+3MKL model. [*See the electronic edition of the Journal for a color version of this figure.*]

X-ray spectrum of central 3 acrimony by XMM-Newton (Takahashi + 2004)

X-ray spectrum is LMXB + 3 hot plasma (kT~ 0.1, 0.3, 0.6 keV)

Galactic Center

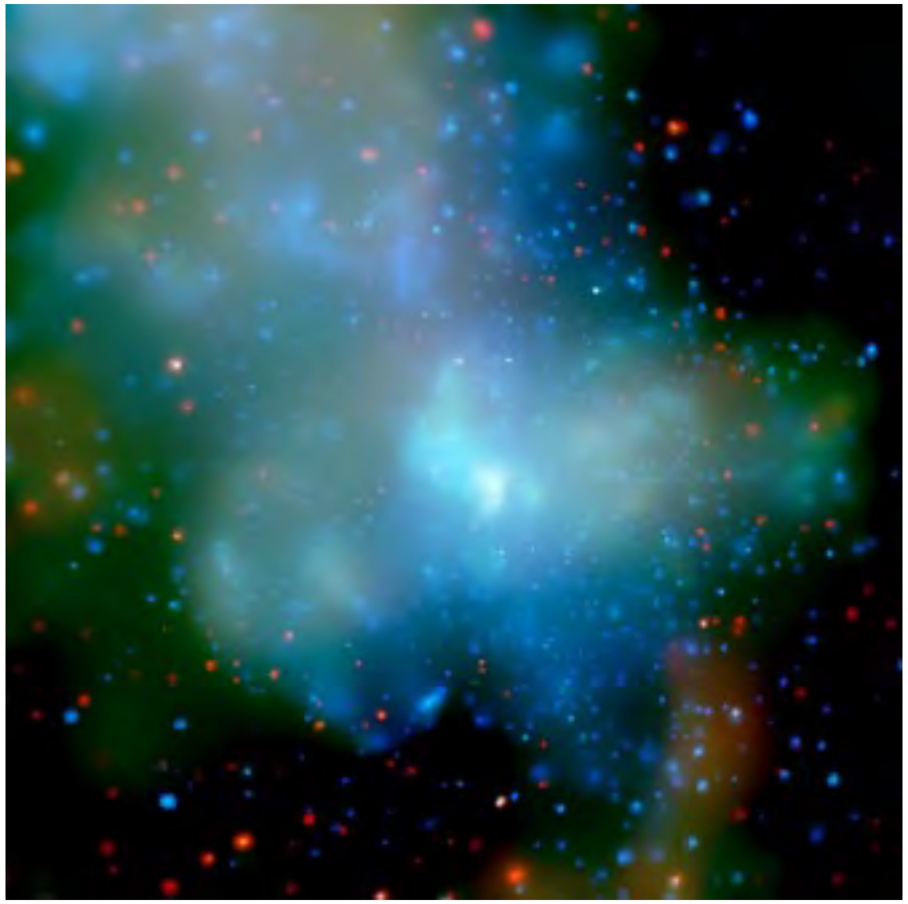

Lots of point sources,
including central AGN and binaries, which are often time-variable.
diffuse emission of thermal and reflecting molecular clouds.(Muno et al. 2008)

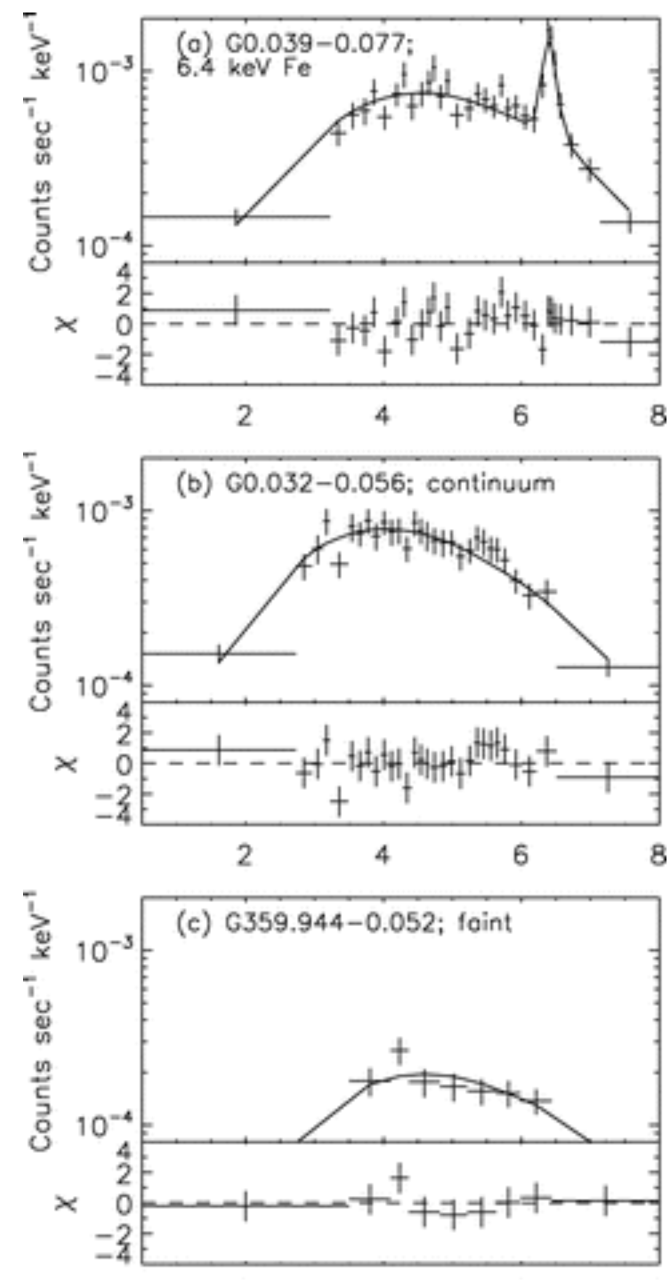

Chandra image of 16 arcmin across
NASA/CXC/UCLA/MIT/M.Muno et al.
Energy (Red: 0.5-2.0 keV; Green: 2.0-4.0 keV; Blue: 4.0-8.0 keV)

The absorbing material is very thick, to be 10^{24} cm^{-2}.

My approaches to DM

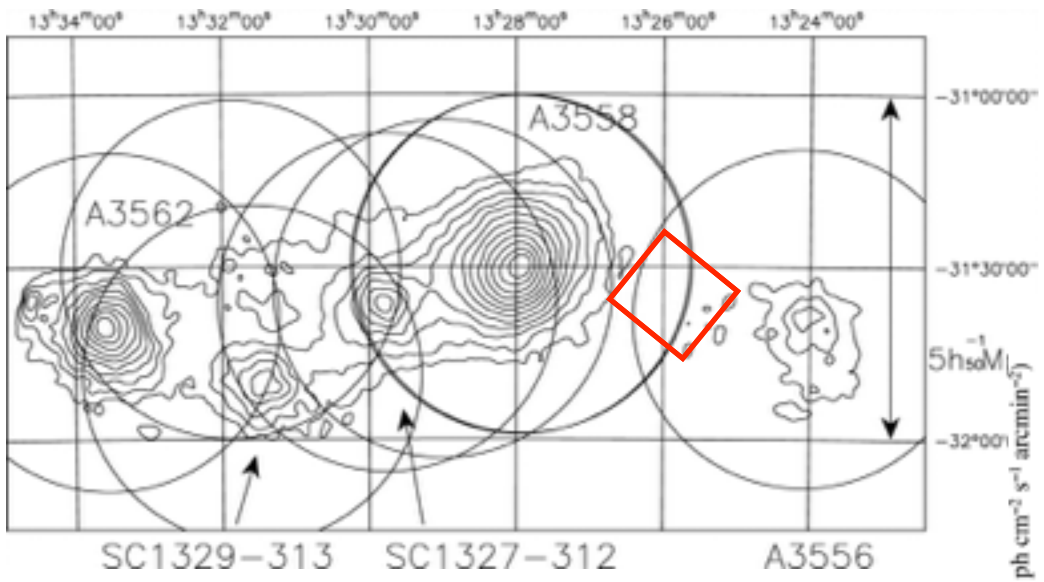

Emission from filaments
(2011+mitsuishi)

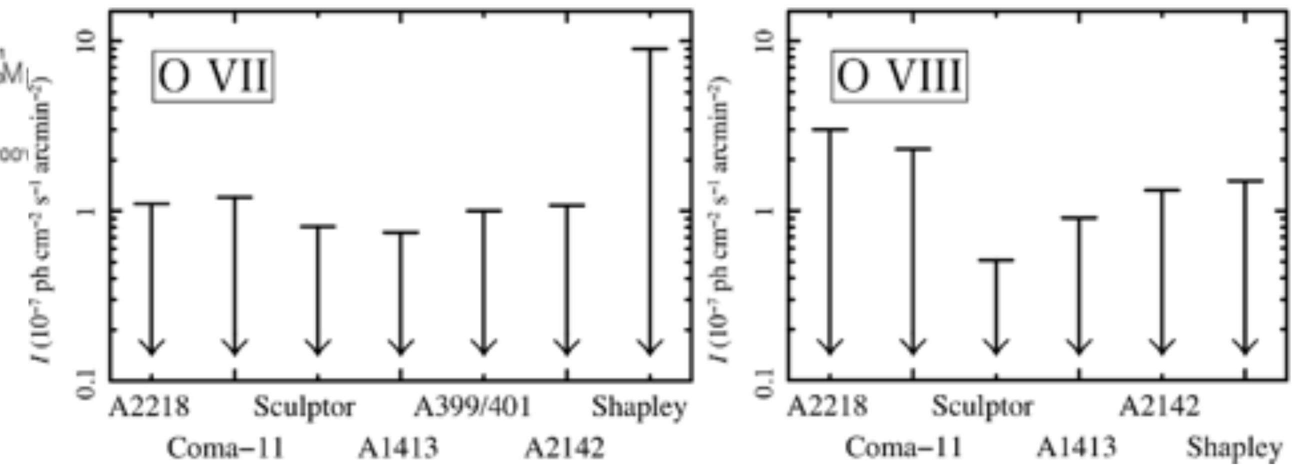

Future mission DIOS to observe the cosmic web (WHIM)

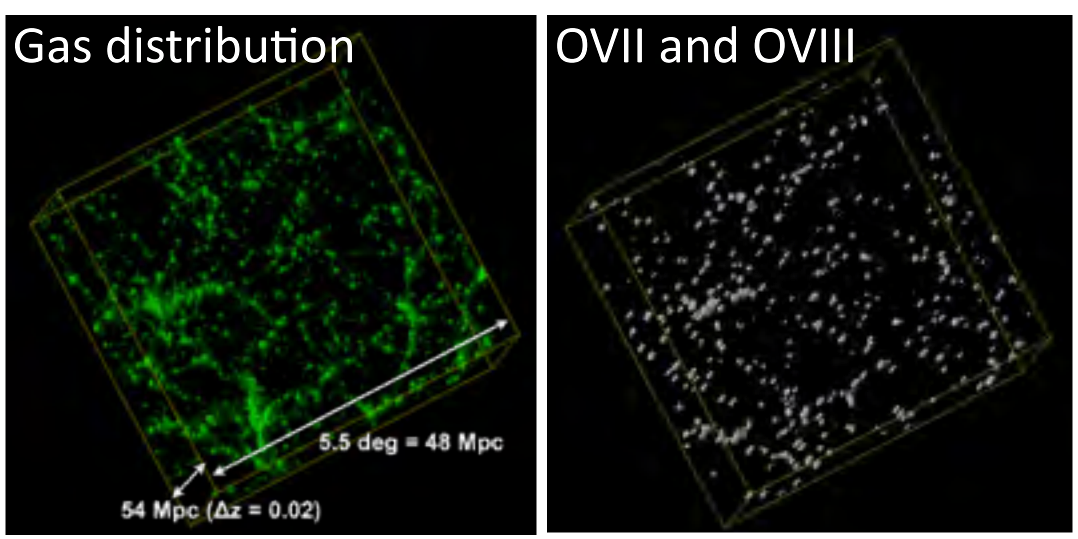

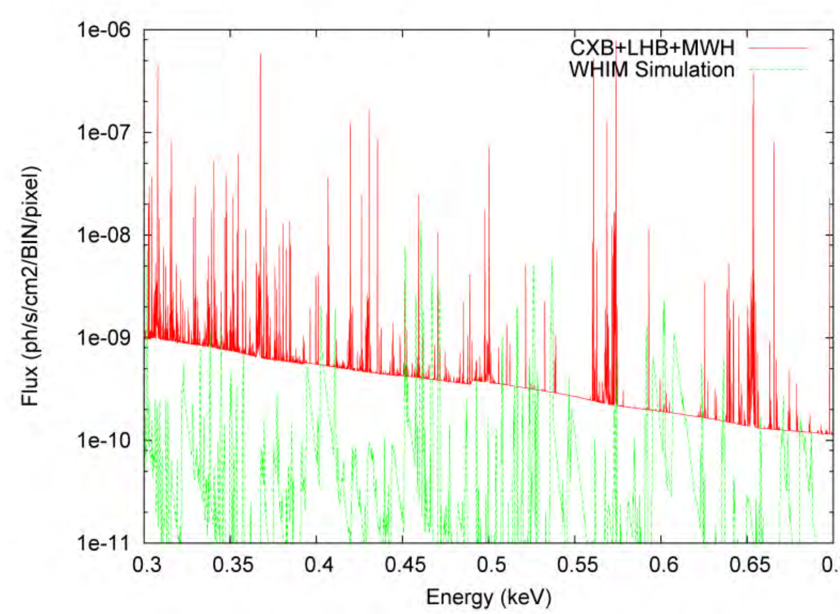

WHIM
Soft X-ray BG

(Yoshikawa+2003,Yoshikawa+2004,Kawahara+2006)

Understanding of “background” emission is essential

Strategy of our study

Strategy to search DM clues

If a line can be detected with "n" σ, it can be written as

$$n = \frac{S}{\sqrt{S+2B}} = \frac{I_S A\Omega T}{\sqrt{(I_S + 2I_B \Delta E)A\Omega T}}$$

$$I_S = \frac{n^2 + \sqrt{n^4 + 8n^2 I_B \Delta E A\Omega T}}{2A\Omega T}$$

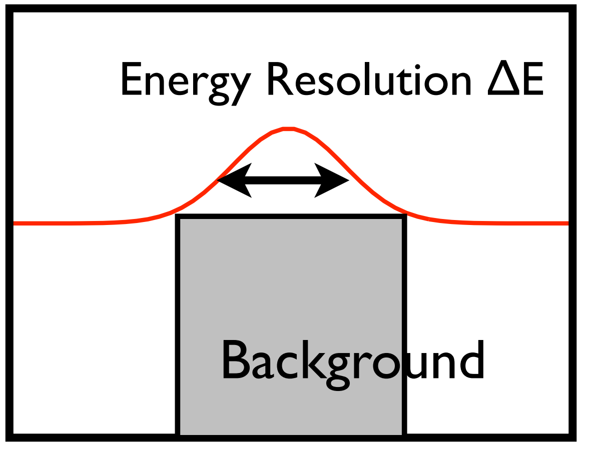

Selection of targets, detectors, and dataset to maximize "n"

1. Target: DM I_S vs "background" I_{B1} emission in fov
2. Detector: Line sensitivity limited by energy resolution ΔE and non-Xray background I_{B2}
3. Dataset: available fov $A\Omega$ and exposure time T

Column density of DM

DM locates in large "gravitational" objects. Such system contains baryons.

	Typical mass	Column density of DM
Rich cluster (Perseus)	$10^{14\text{-}15}M_\odot$	100-1000 $M_\odot/pc^2$
Galaxy (M31/GC)	$10^{11\text{-}12}M_\odot$	200-600 $M_\odot/pc^2$
Our Galactic halo or "X-ray Diffuse Backgrouund (XDB)"	$(10^{11}M_\odot)$	50-100 $M_\odot/pc^2$
Dwarf galaxy	$>10^9M_\odot$	50-100 $M_\odot/pc^2$

see ex.Boyarsky + 2010,2014

DM column density of Milky way estimated by rotation curve and NFW profile parameters (Sofue+2012)

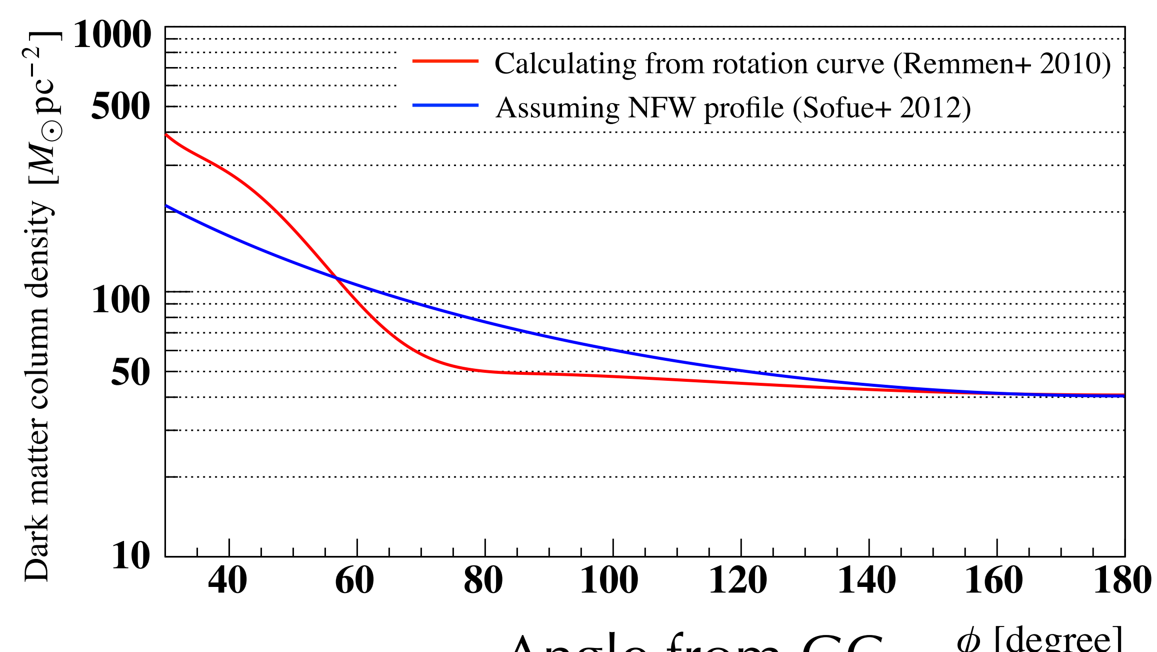

Angle from GC

X-ray background

X-ray background spectrum
Sum of AGN (extragalactic) +
Galactic hot halo +
Local (~ neighborhood of the Solar system)

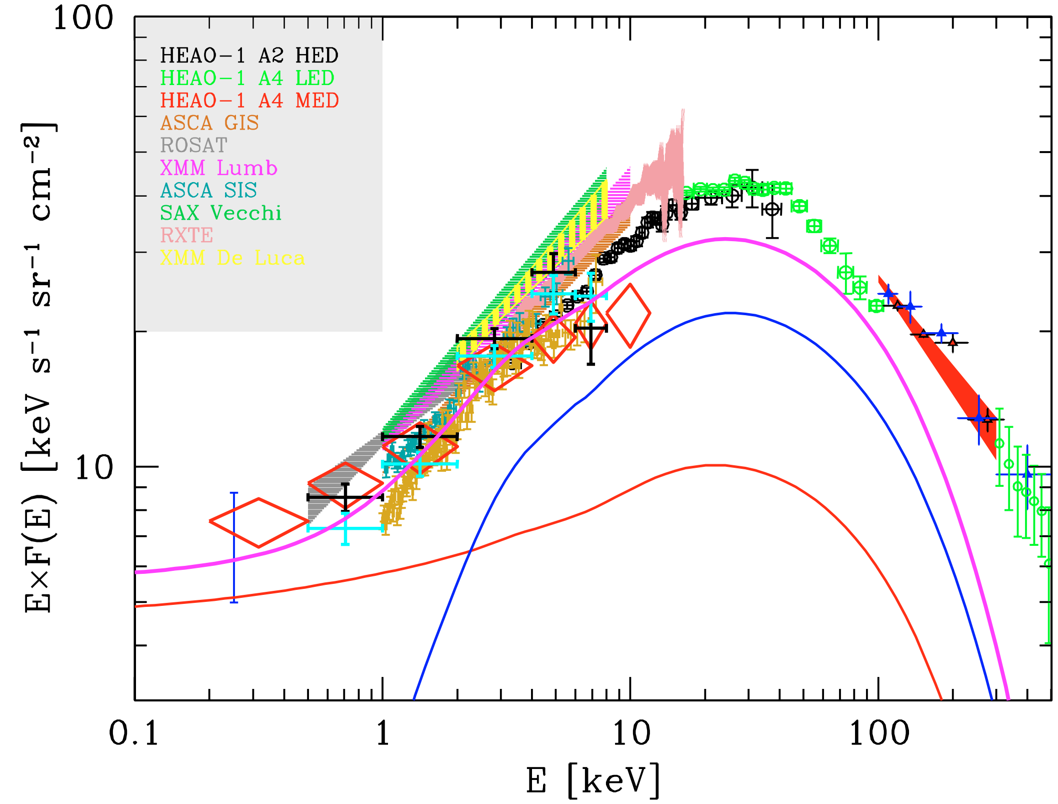

Rosat 1/4 keV band image

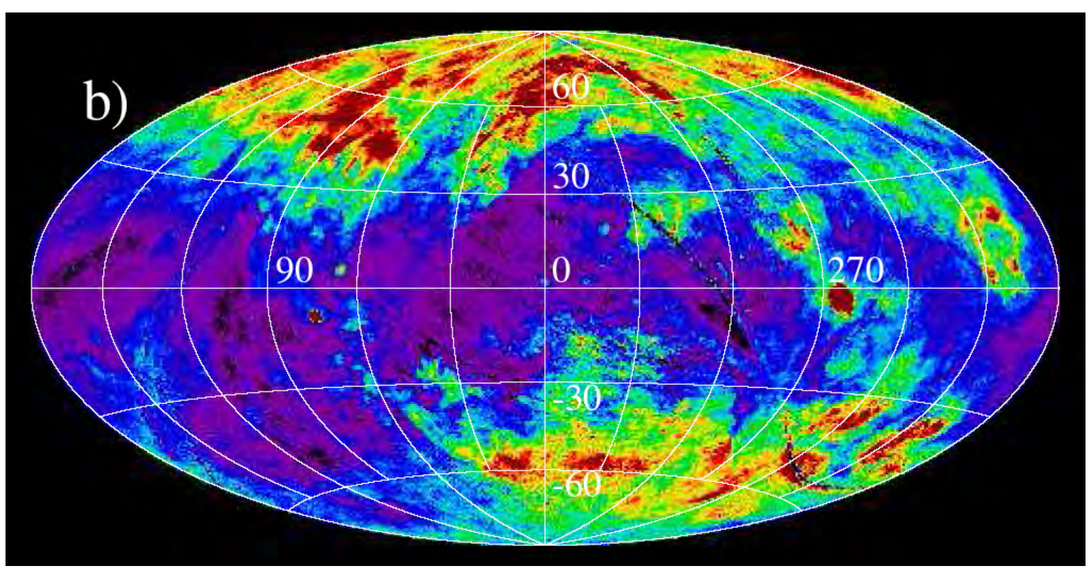

Rosat 3/4 keV band image

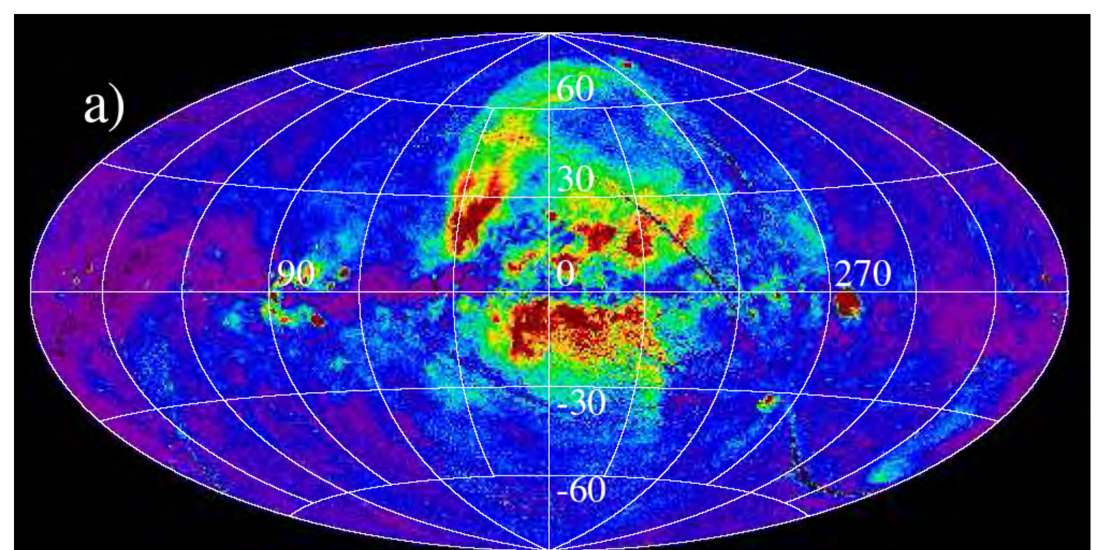

X-ray spectrum of the Galactic halo

The Galactic halo spectra is well represented by Suzaku.

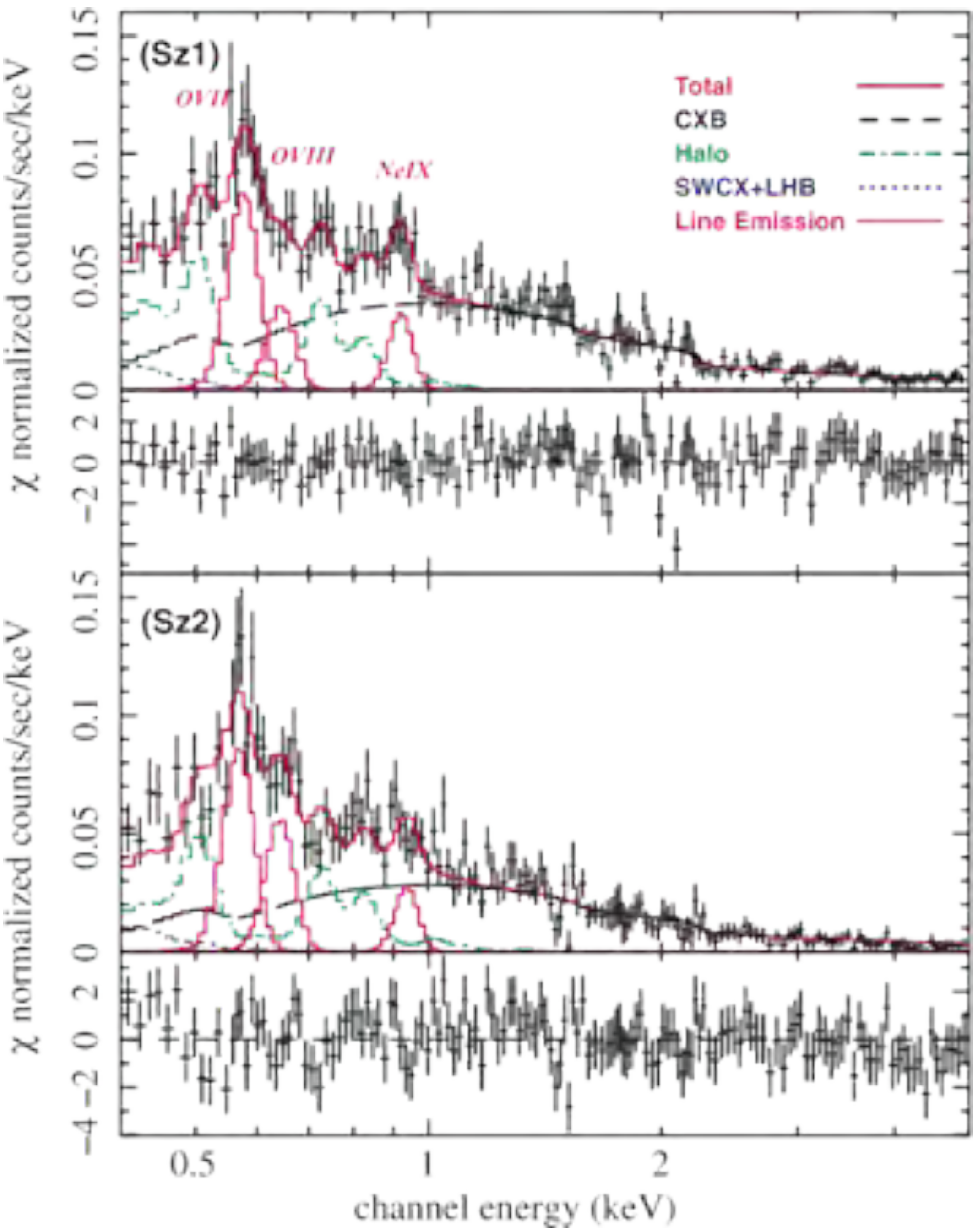

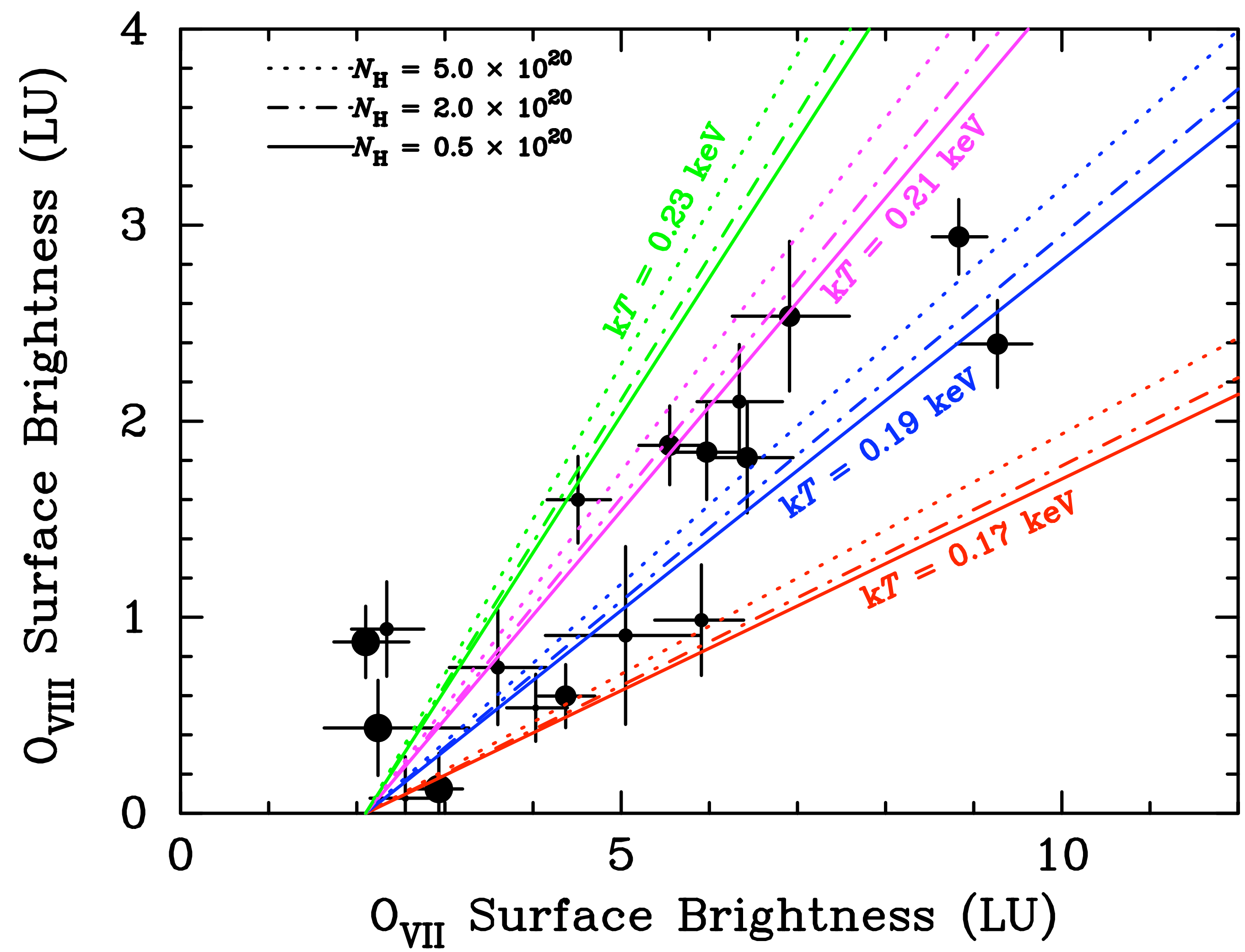

Yoshino+2009, Hagihara+ 2010

Line Sensitivity by X-ray CCD

Emission model

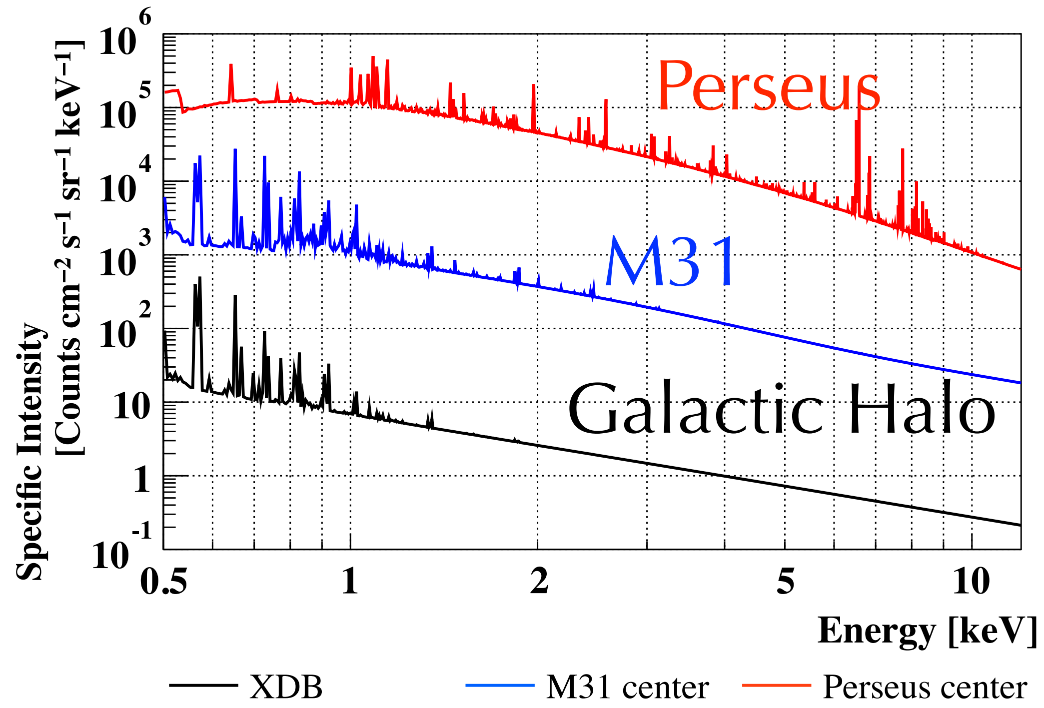

Line sensitivity with ΔE~ 100eV, T=100 ksec, Ω=3x3 arcmin^2

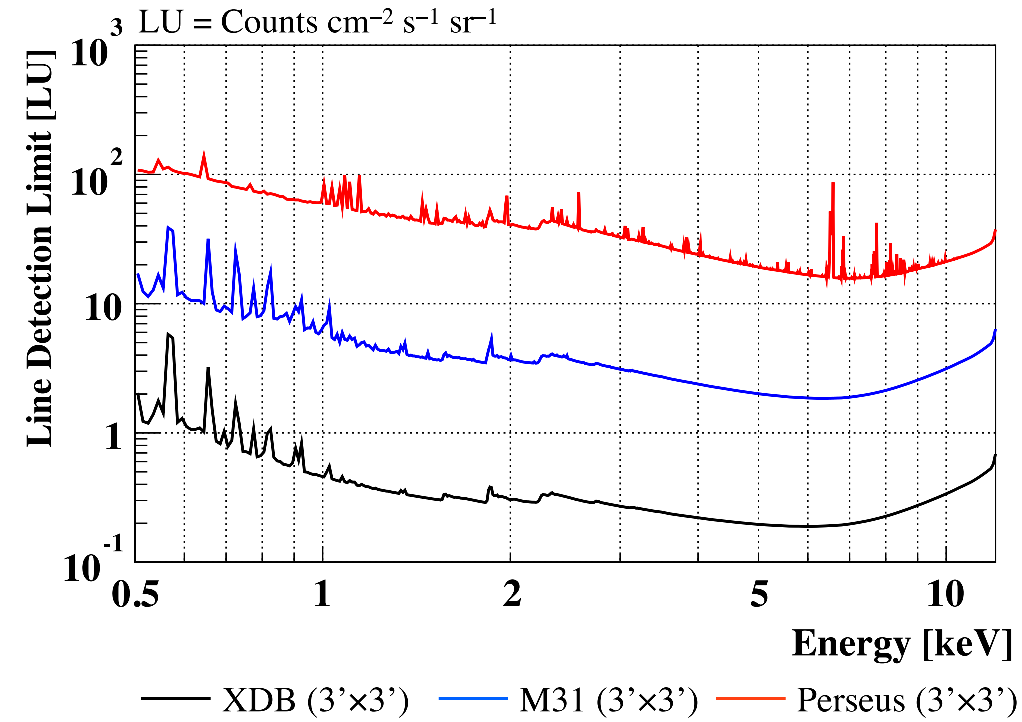

Line sensitivity/DM column density

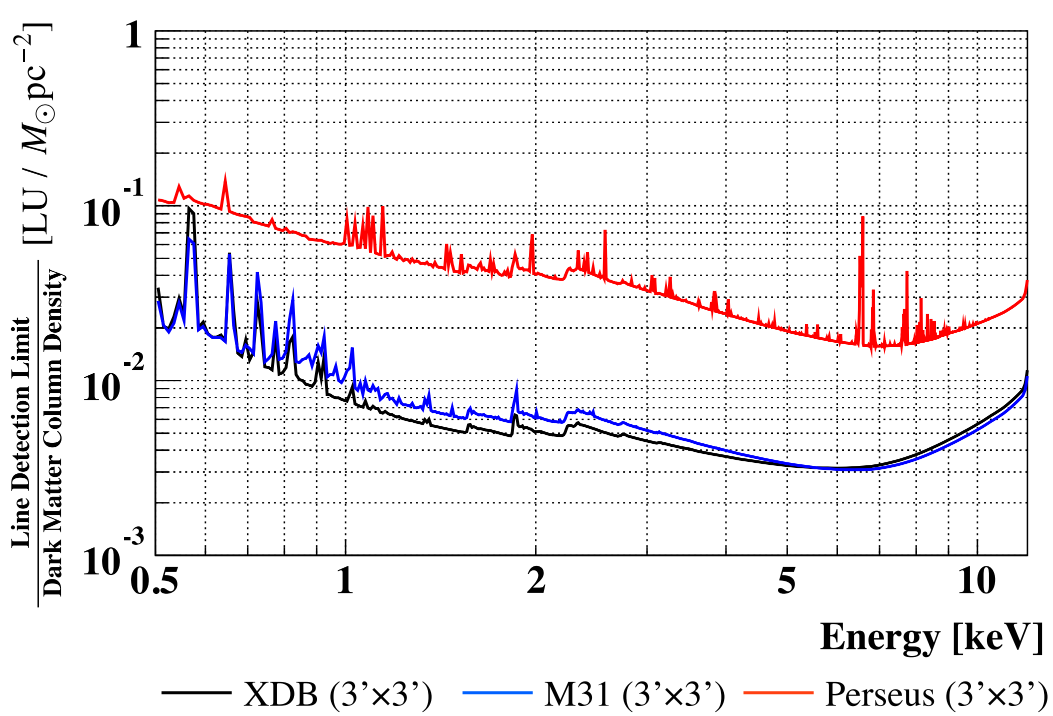

M31 and Galactic halo can give better sensitivity. (Cluster is too bright in X-ray, even though it contains more DM.)

Exposure for the Galactic halo can be larger than that for M31.

Current X-ray observatories



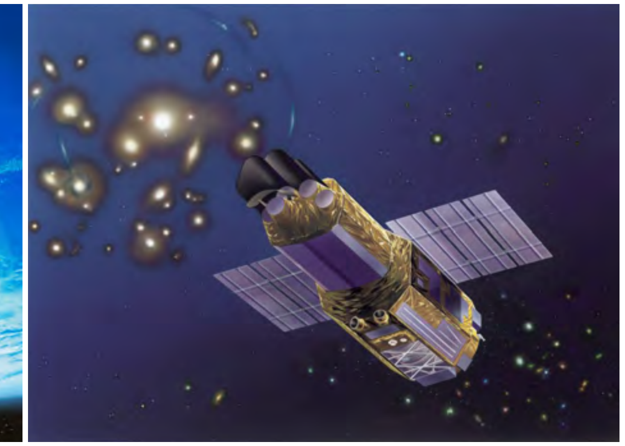

	Chandra/ACIS	XMM-Newton/PN, MOS	Suzaku/XIS
fov (arcmin^2)	8.3x8.3x(4FI+6BI)	700 (2MOS+PIN)	17.8x17.8(3FI+1BI)
Energy band (keV)	0.3-12	0.15-15	0.2-12
Energy resolution (eV)	50-200	50-200	50-200
Effective area (cm^2)	200 (4FI), 400 (6BI)	800 (2MOS), 1200 (PN)	660 (3FI), 320 (BI)
NXB (cm^{-2}s^{-1}sr^{-1} keV^{-1})	10-1000 (unstable)	5-100 (unstable)	1-10 (stable)
Orbit	133000 km x 16000 km	114000 km x 7000 km	Low Earth (550 km)

Comparison of X-ray observatories

AΩ(area x fov)

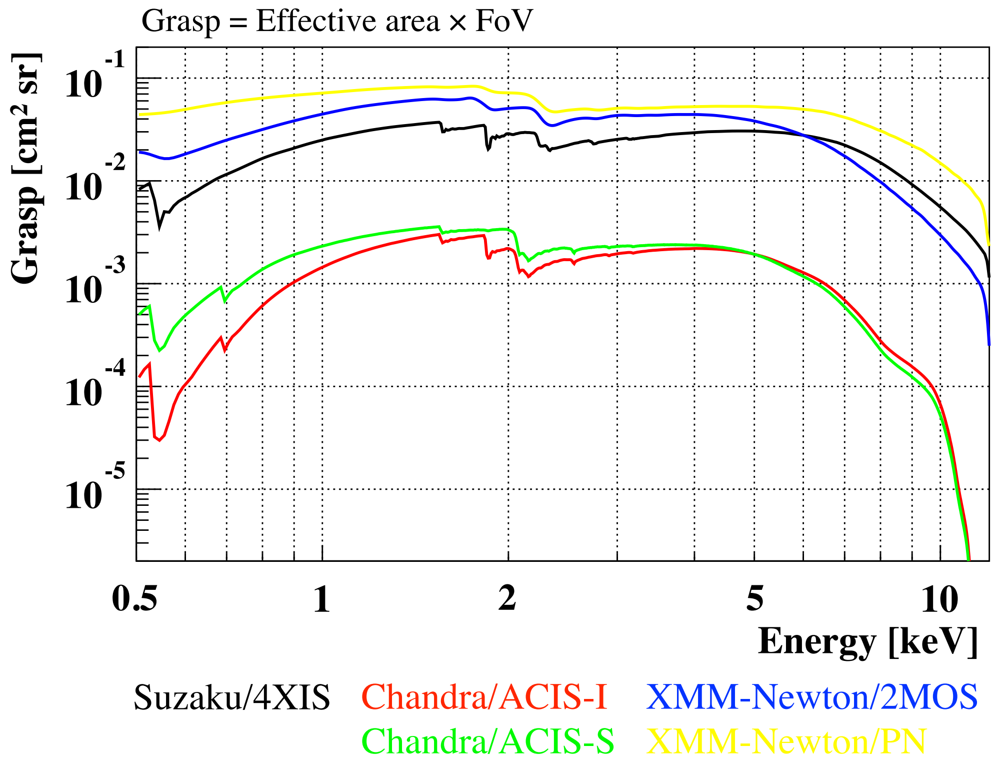

Typical non X-ray background

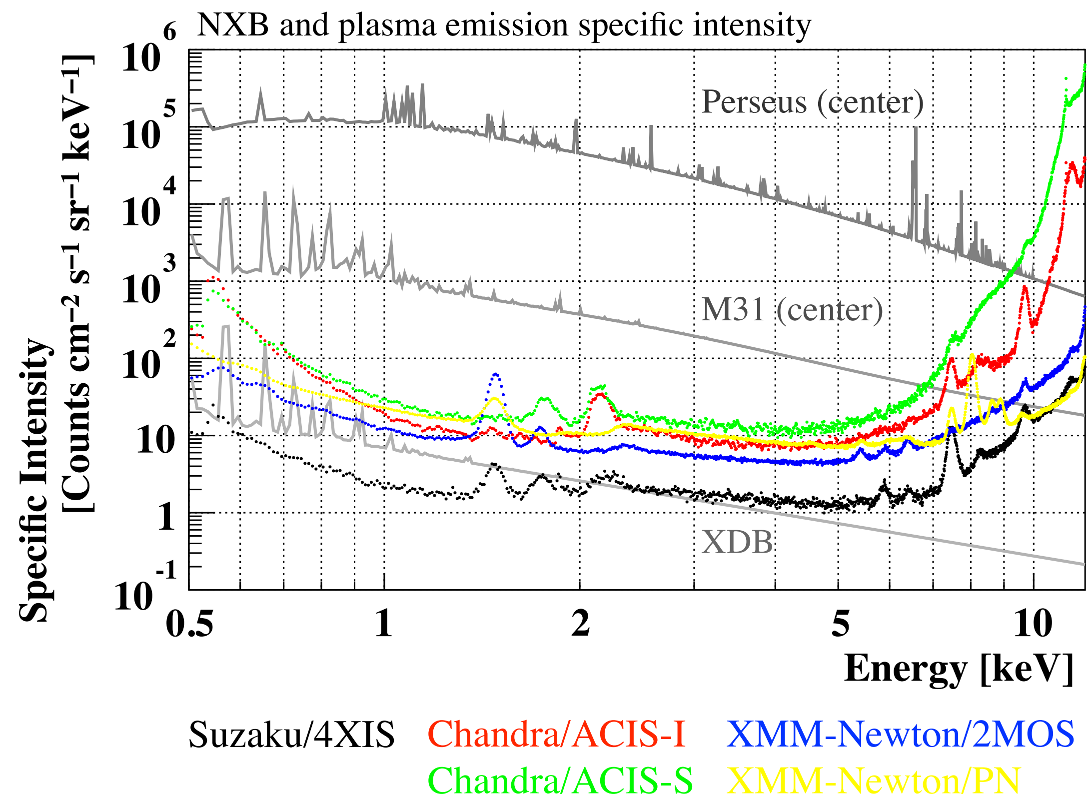

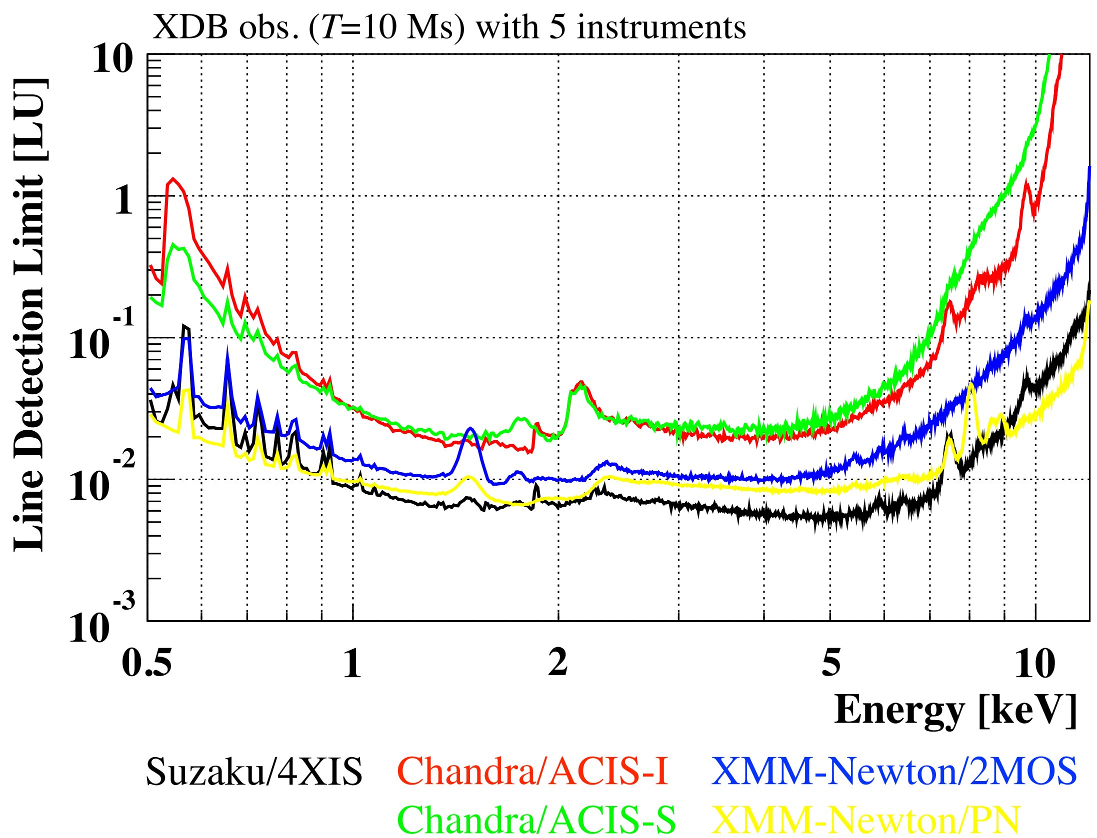

NXB of Suzaku is comparable to XDB, but others are above XDB and variable. i.e. XDB observation is not photon limited. Reproducibility of NXB is important.

Analysis details

Suzaku analysis of the Galactic halo

Sekiya et al. PASJ, accepted (2015)
(arXiv:1504.02826)

1. Data selection from the archive
   i) Data screening to obtain stable background
      a. Solar wind charge exchange emission
      b. Fluorescent lines from the Earth atmosphere
      c. Low Non-X-ray background
   ii) Remove point sources
2. Reproduction modeling of the “Soft X-ray Background”
3. Systematic errors and its origins
4. Obtained upper limits for unknown emission lines
5. LEE correction
6. Constraints on sterile neutrino

Data selection from Suzaku archive

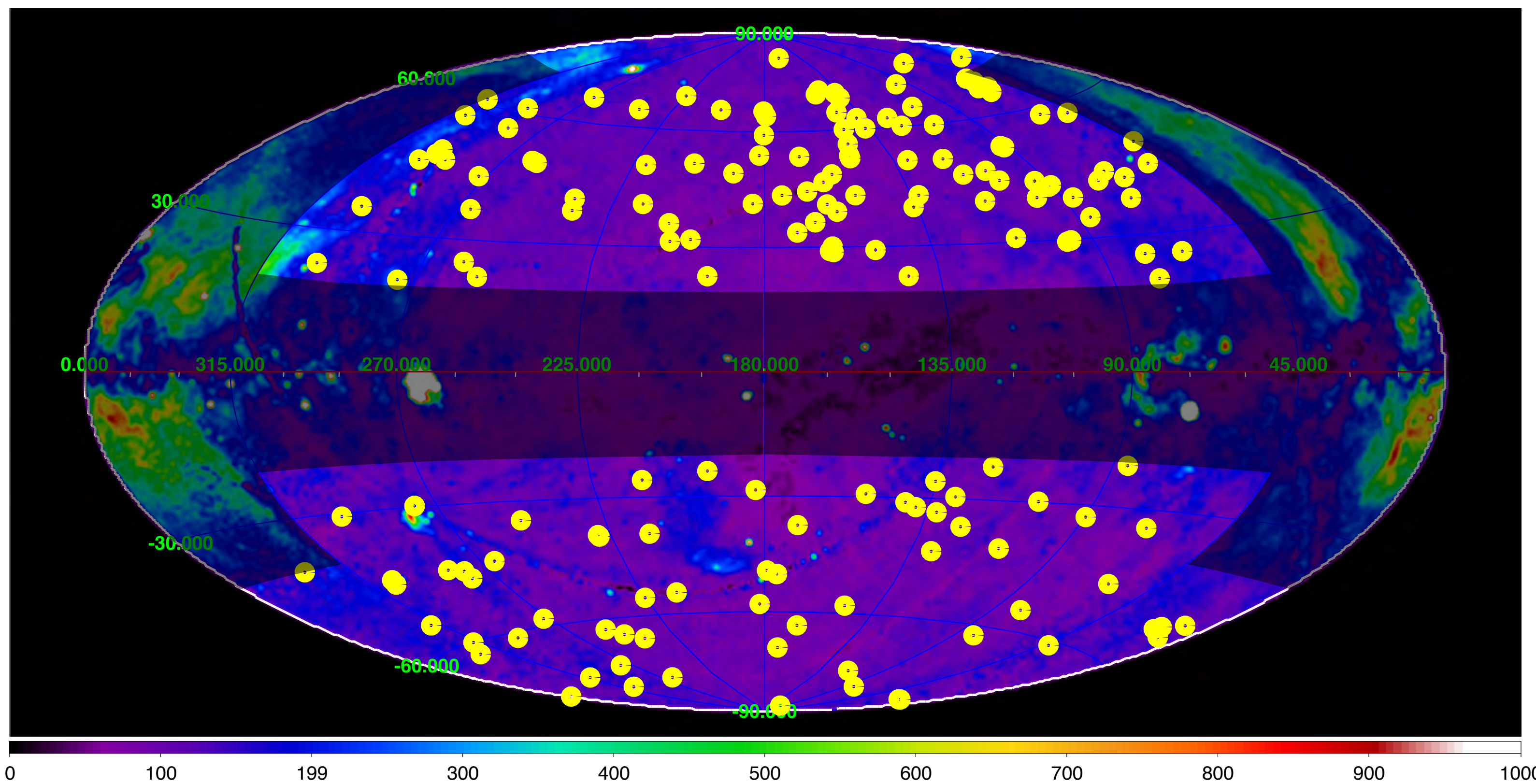

Galactic coordinate centered on the "Anti-Center"

187 dataset with total from Suzaku archive

- XIS (CCD) nominal clocking mode
- No bright sources or diffuse emission structure
  - |b|>20° to avoid Galactic plane emission
  - Separate from North Polar Spur

Mask point sources

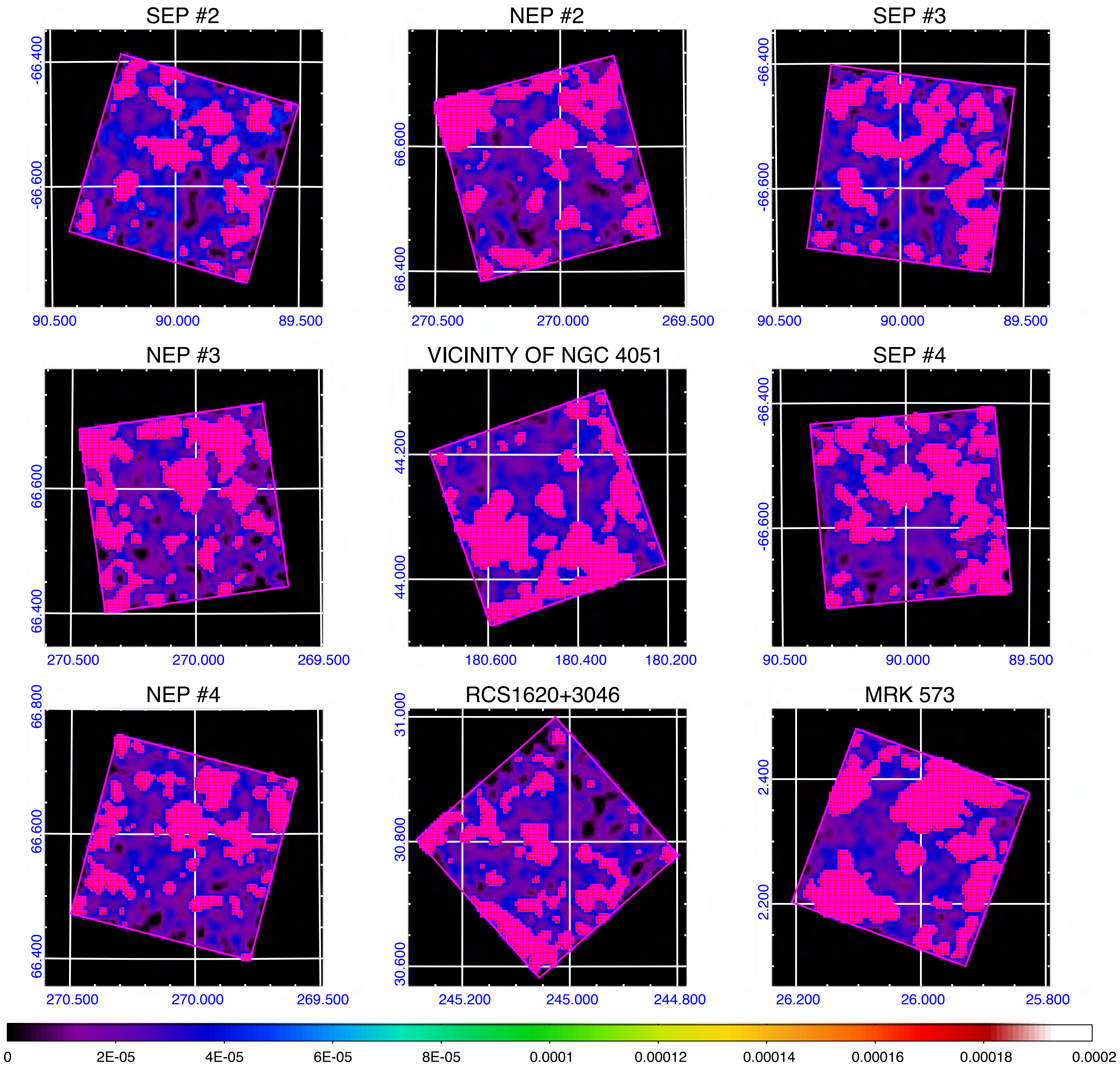

Magenda regions are excluded to remove source confusion.

Data Screening

A sample of GTI (Good Time Interval) to cut Solar wind charge exchange

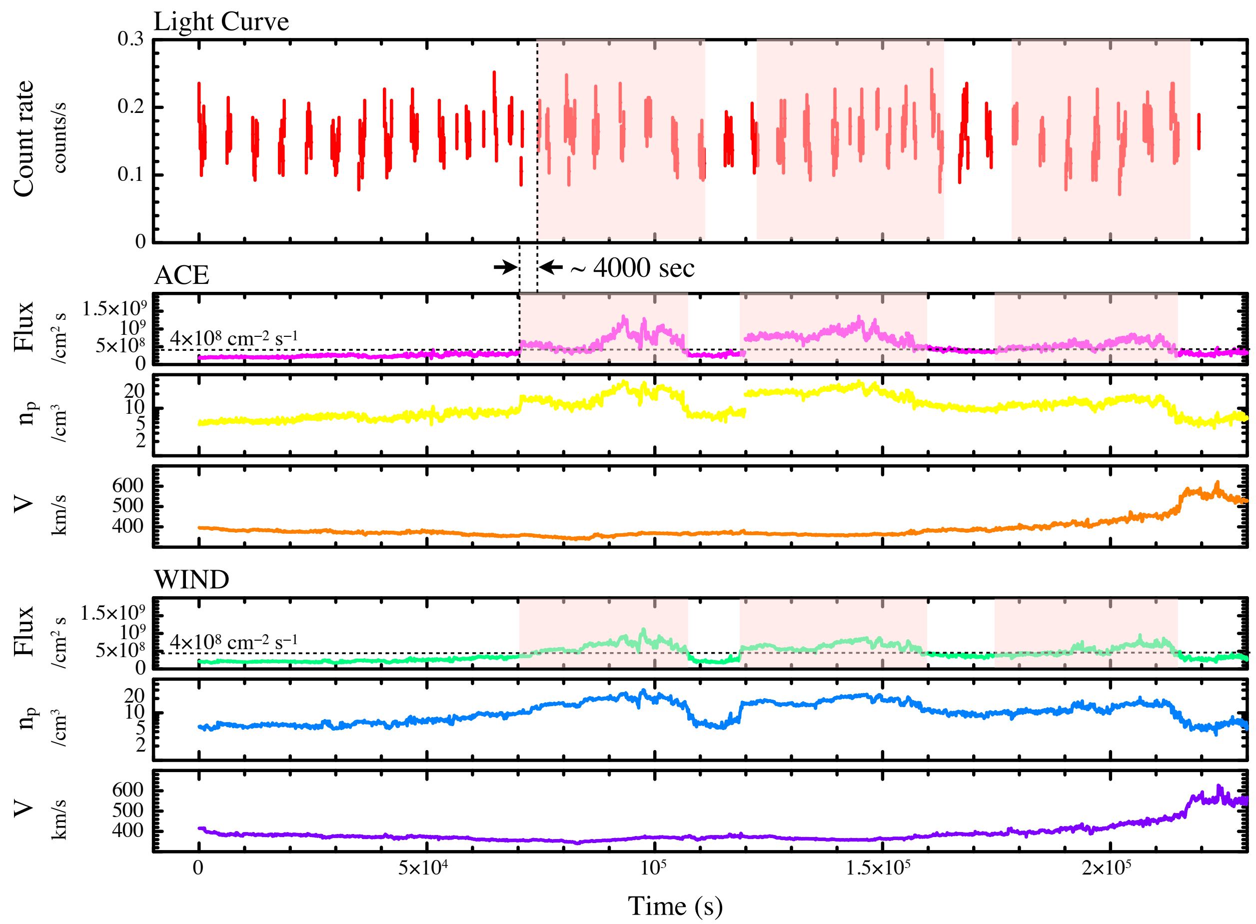

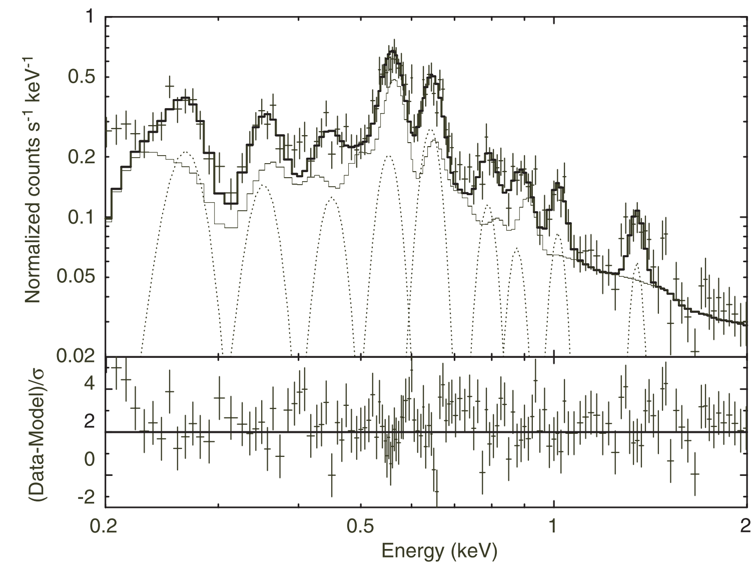

Line emission during Solar flare
From Fujimoto et al. 2006

Avoid South Atlantic Anomaly and COR < 8 GV/c⇒Low CR background

Remove low elevation data from the Earth limb ⇒Fluorescence (See Sekiya+2015)

⇒Total 31.5 Msec data , $2\text{x}10^6$ photons

Soft X-ray Background

(1) Heliospheric charge exchange (OVII Ly γ)
(2) Local hot bubble (kT ~ 0.1 keV plasma)
+[(3) Galactic Halo Emission (kT ~ 0.2 keV + >0.4 keV plasma)
+(4) Cosmic X-ray Background (photon index ~1.4)]*ISM absorption
(see Yoshino et al. 2008)

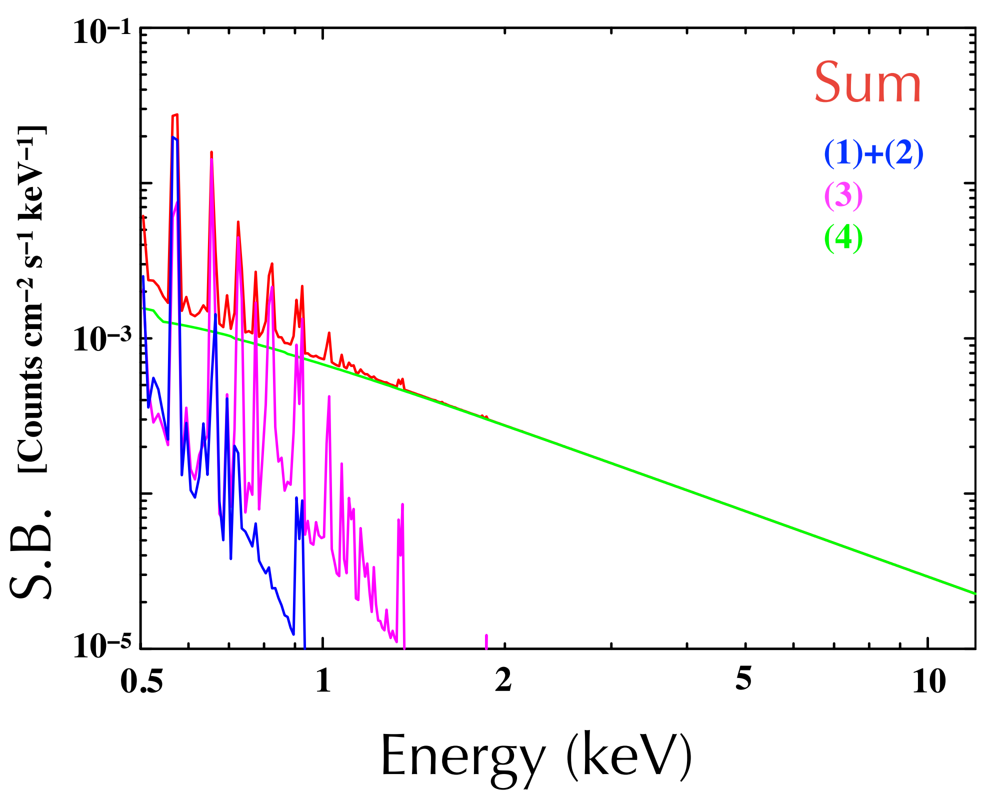

Detector effective area

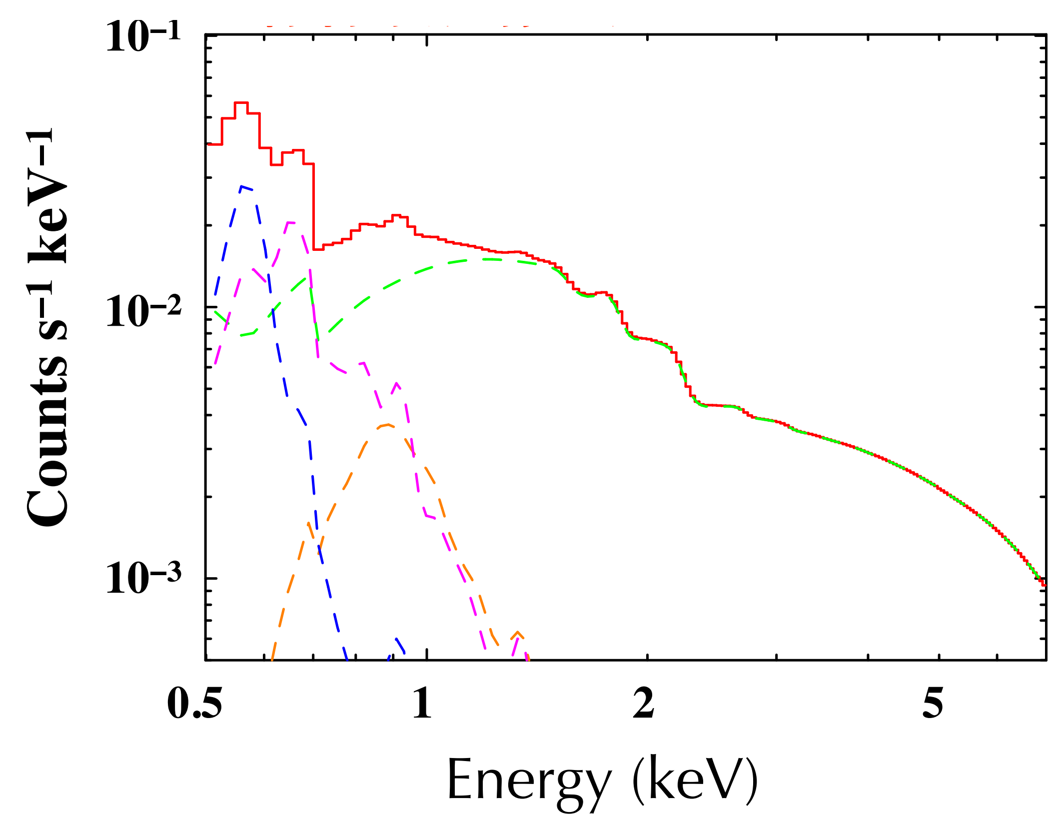

Correction of responses

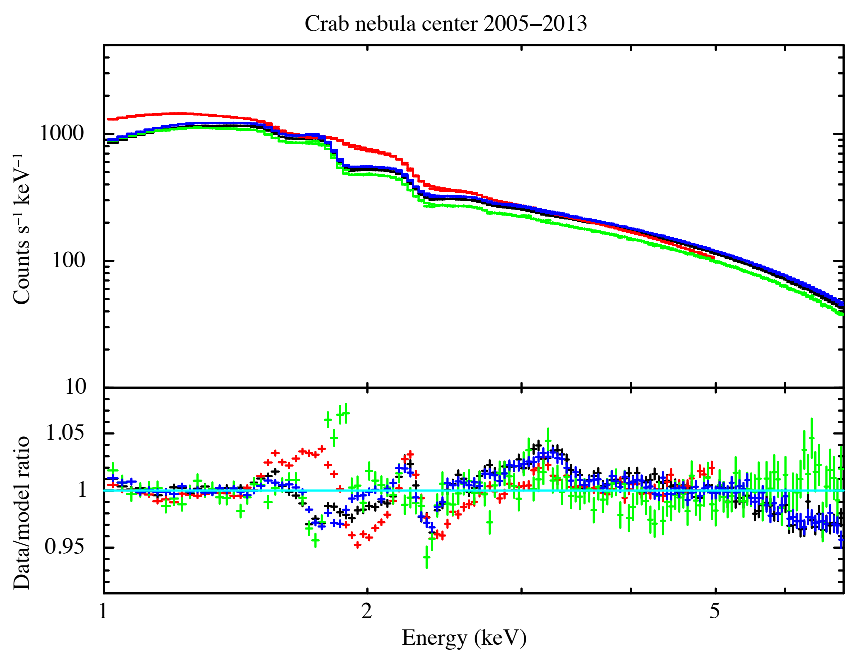

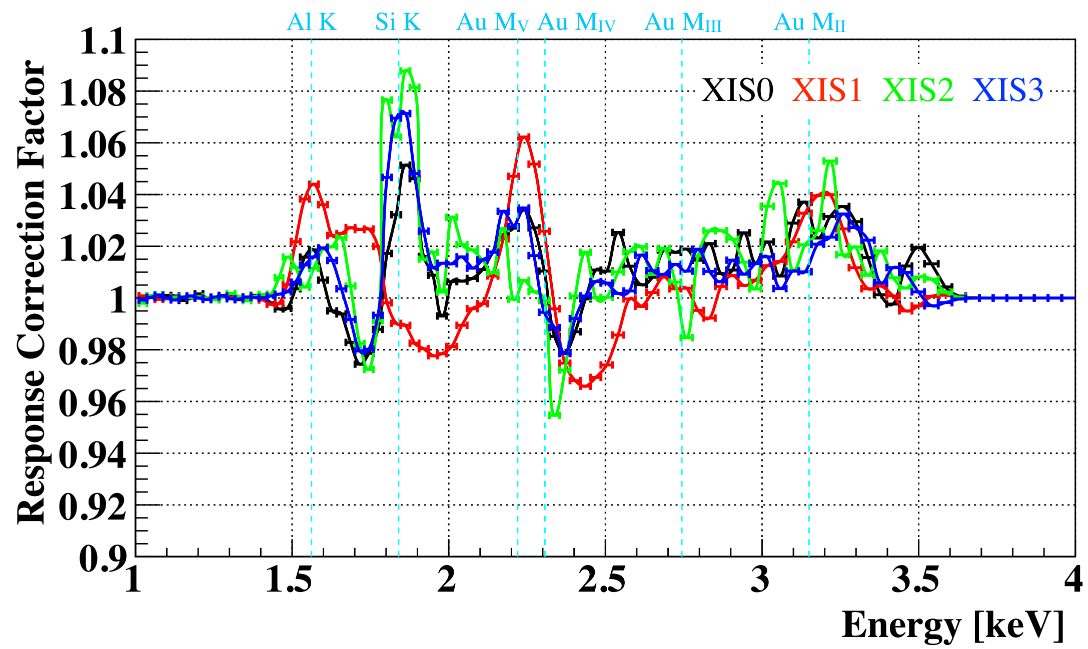

Crab Nebula (Brightest SNe in X-ray sky, and featureless synchrotr
emission) calibration in every year ⇒Residuals < 8%

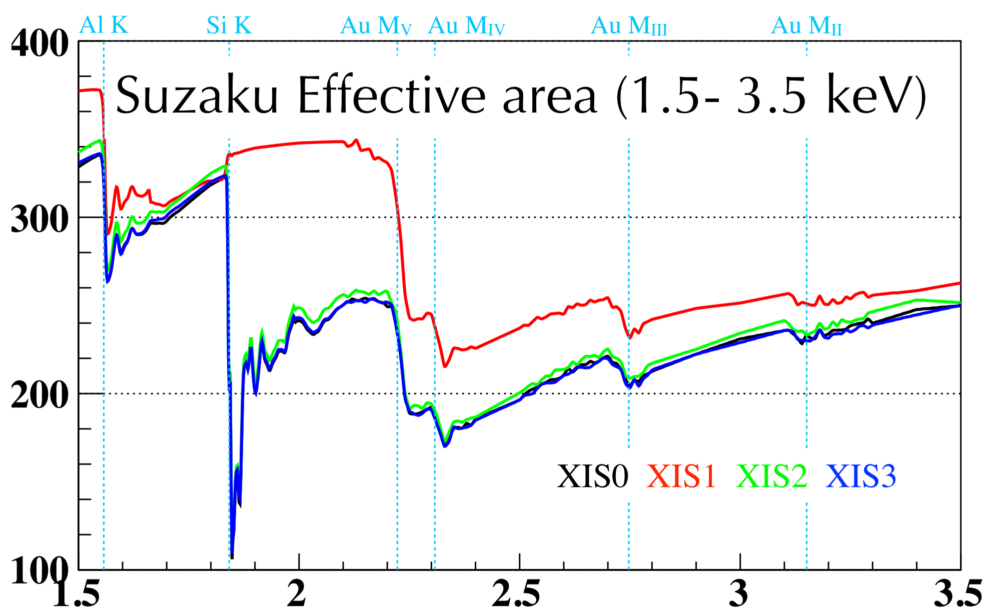

It might come from complex structure due to Au-M edge structure on mirror reflectivity and quantum efficiency of CCD. ⇒The effective area were tuned by these residuals.

Reproduction of NXB

Suzaku NXB is very low and stable.
Usually, it is estimated by "night Earth" database within a few % (Tawa et al. 2008).

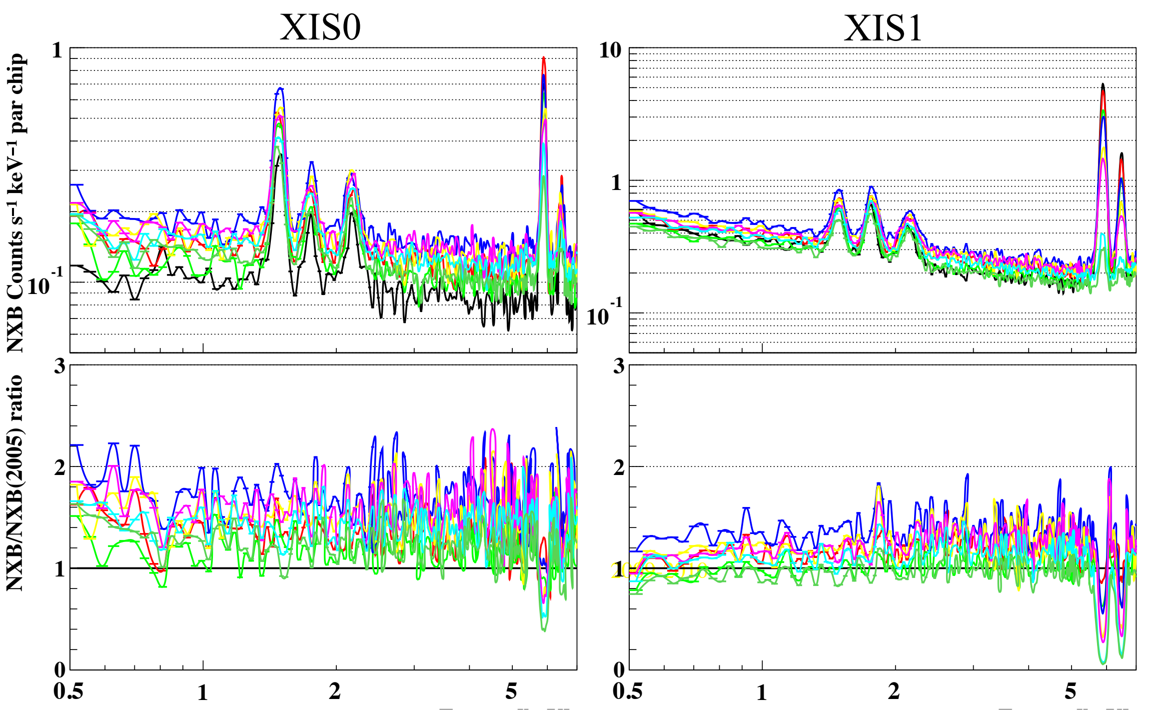

Table 4.4 Instrumental line emission below 7.0 keV (Tawa et al., 2008).

Line	Energy [keV]	Origin
Al-Kα	1.486	OBF, housing, alumina substrate of XIS
Si-Kα	1.740	XIS
Au-Mα	2.123	Housing, XIS substrate, heat-sink
Mn-Kα	5.895	Calibration source
Mn-Kβ	6.490	Calibration source

Improved the reproducibility by direct fitting of background lines

Modeling of "background" emission

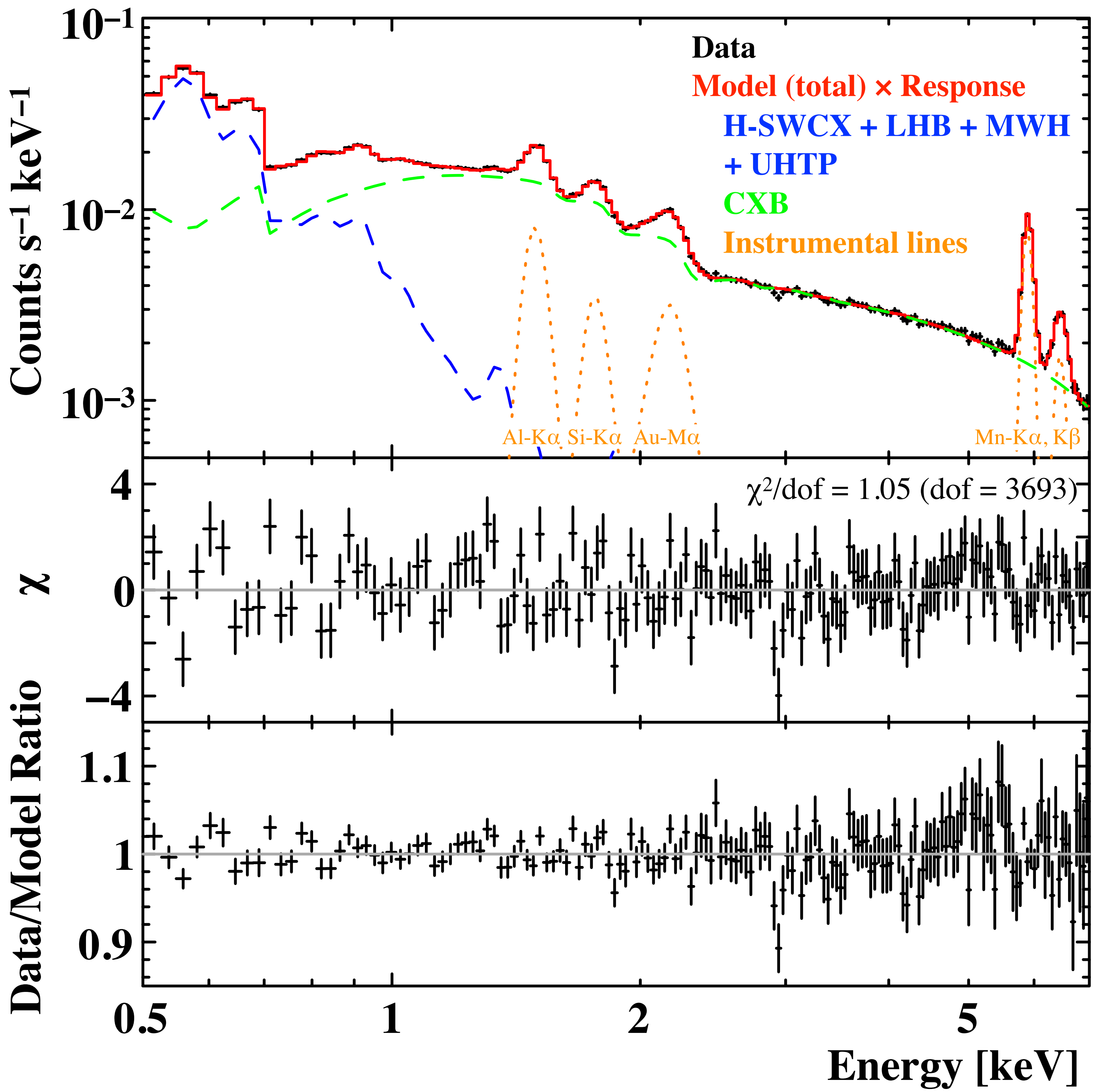

The data are well represented by AGN + Galactic halo + NXB

p-value of 2.5%⇒acceptable fit

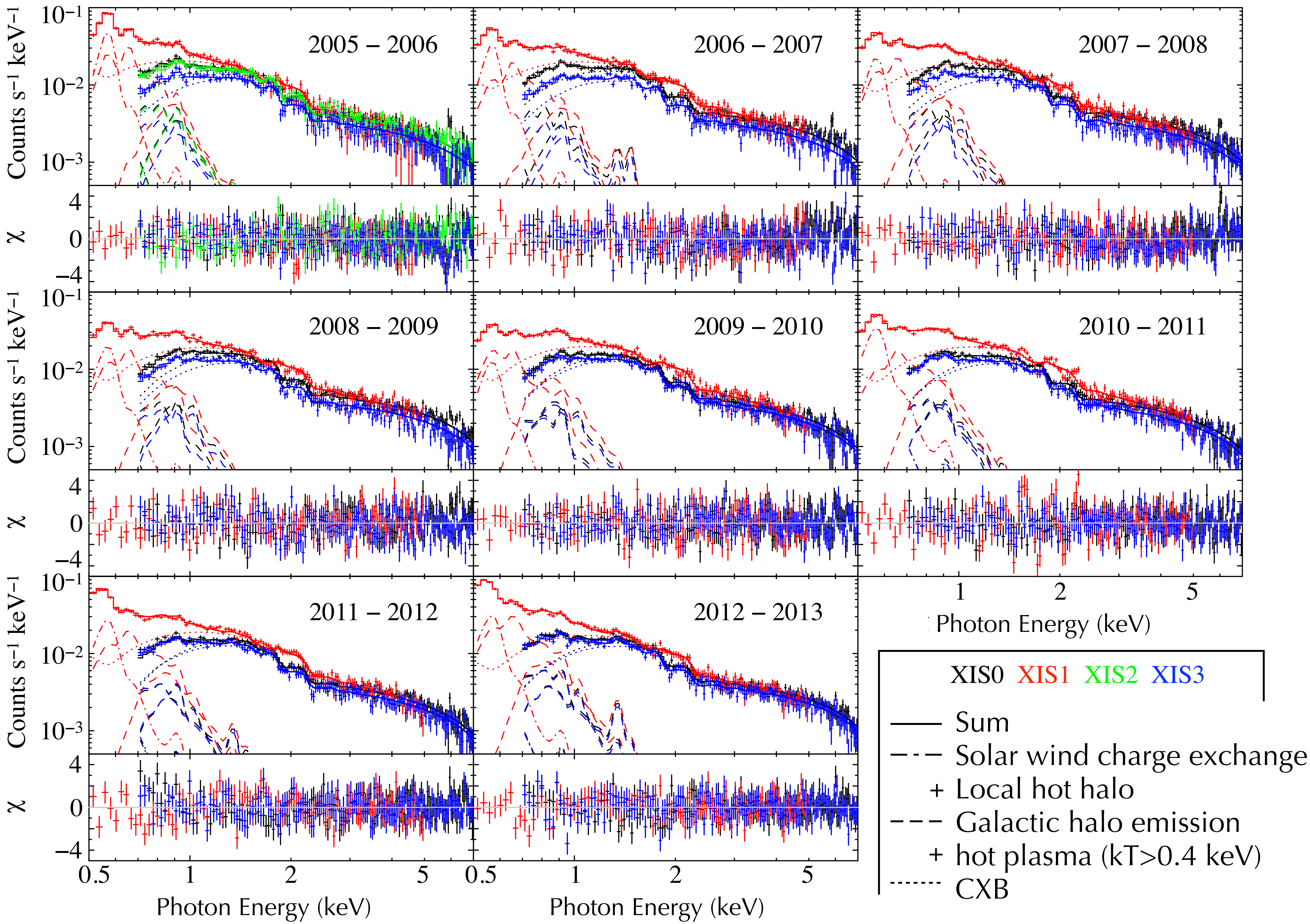

We cross-checked the data by original 187 data set and annual dataset

Statistical limits for unknown emission line

Add a line at every 25 eV with σ=0 eV between 0.5 and 7 keV, and obtain allowed intensity or upper limits.

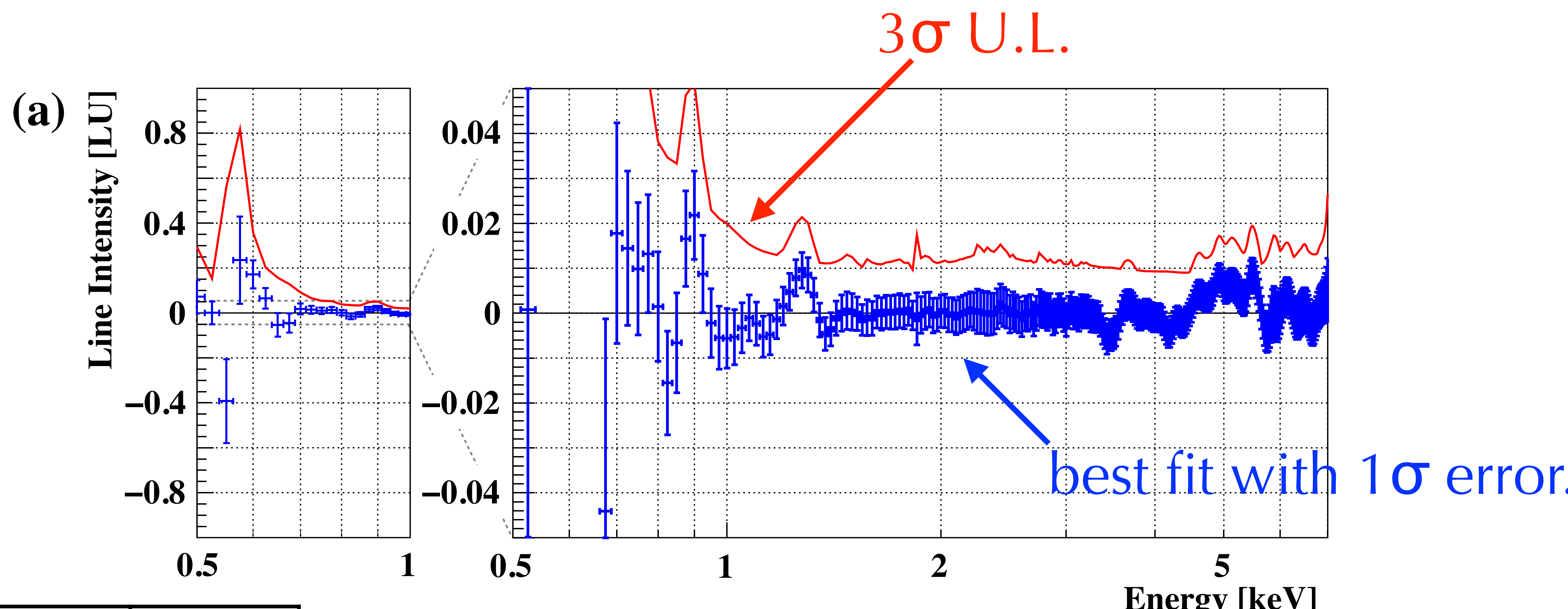

0.600 keV	2.8σ
0.900 keV	2.2σ
1.275 keV	2.4σ
4.925 keV	2.8σ
5.475 keV	2.4σ

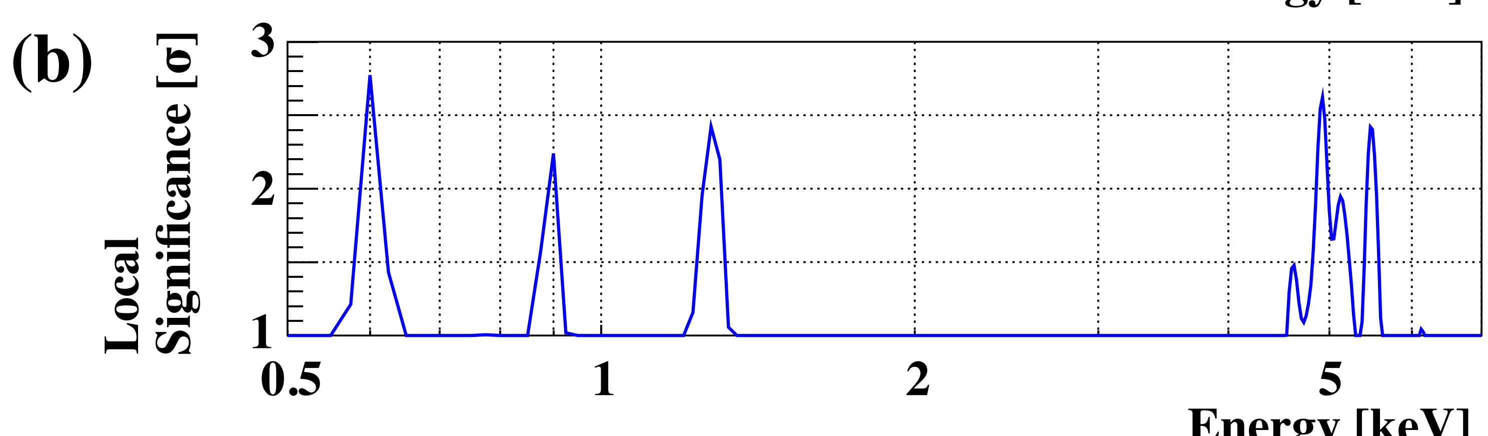

Be careful! it is not the final conclusion.

Systematic errors

- Reproductivity of the background emission
  - Check fitting errors and model uncertainty (mainly the metal abundance of the hot plasma) ⇒small effect

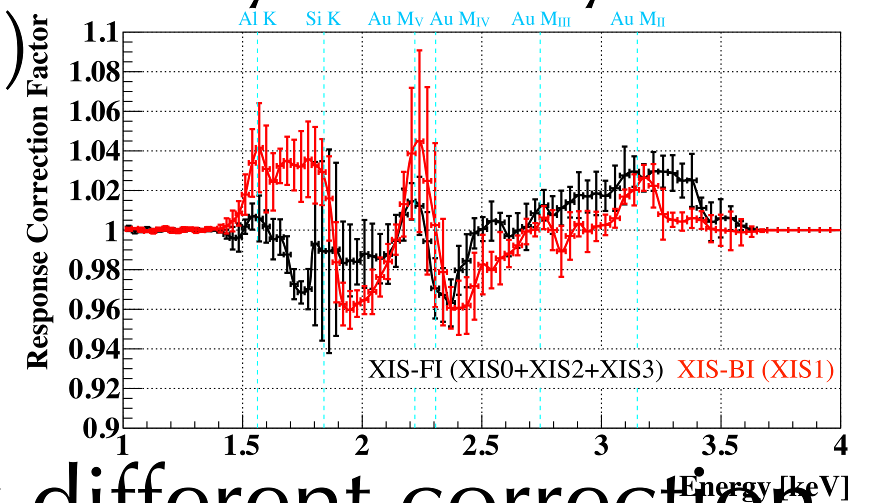

- Response uncertainty
  - Check Crab nebula fit error, and try different correction factor within errors ⇒2~6x10^{-3} LU between 1.5-3.5 keV

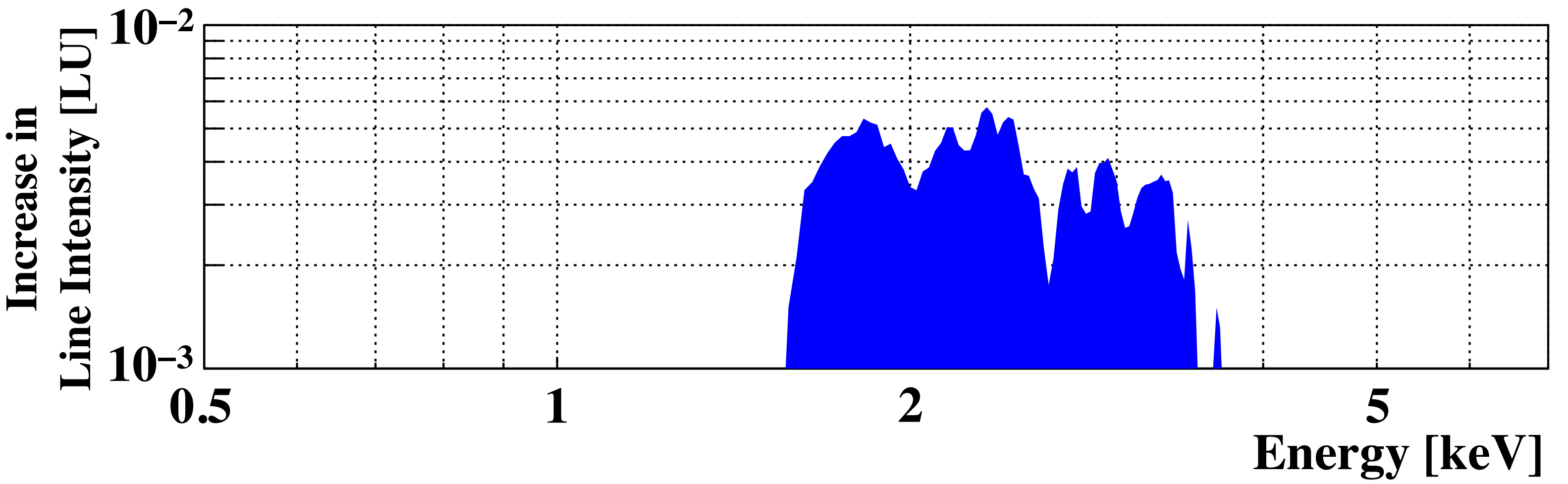

Systematic errors (cont.)

- NXB uncertainty
  - Put maximum/minimum allowable NXB
  - Fit NXB lines in 187 (unstacked) dataset, and check the deviation

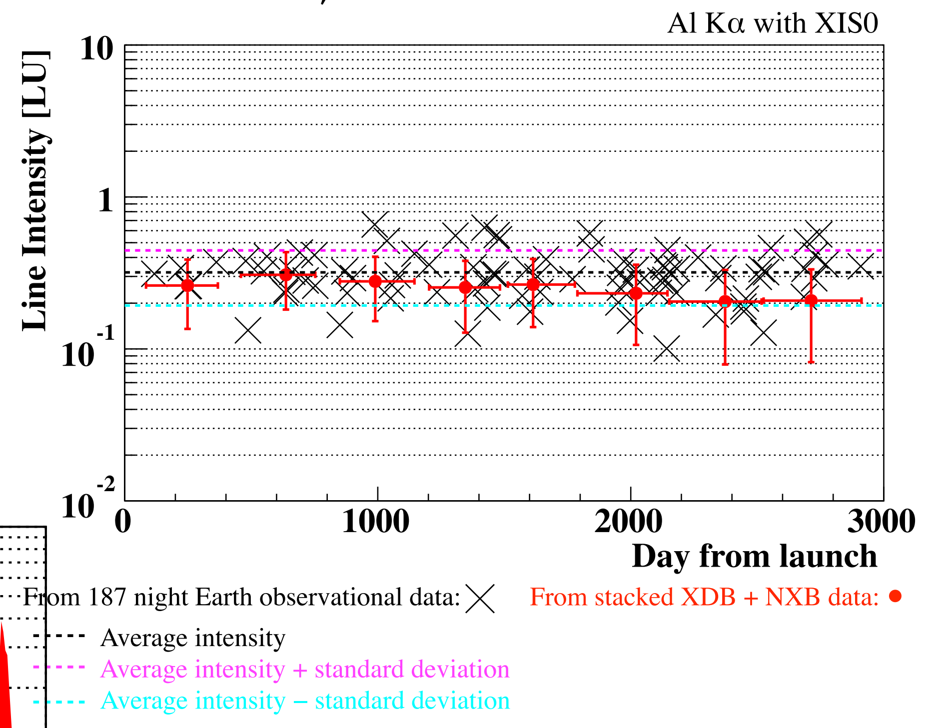

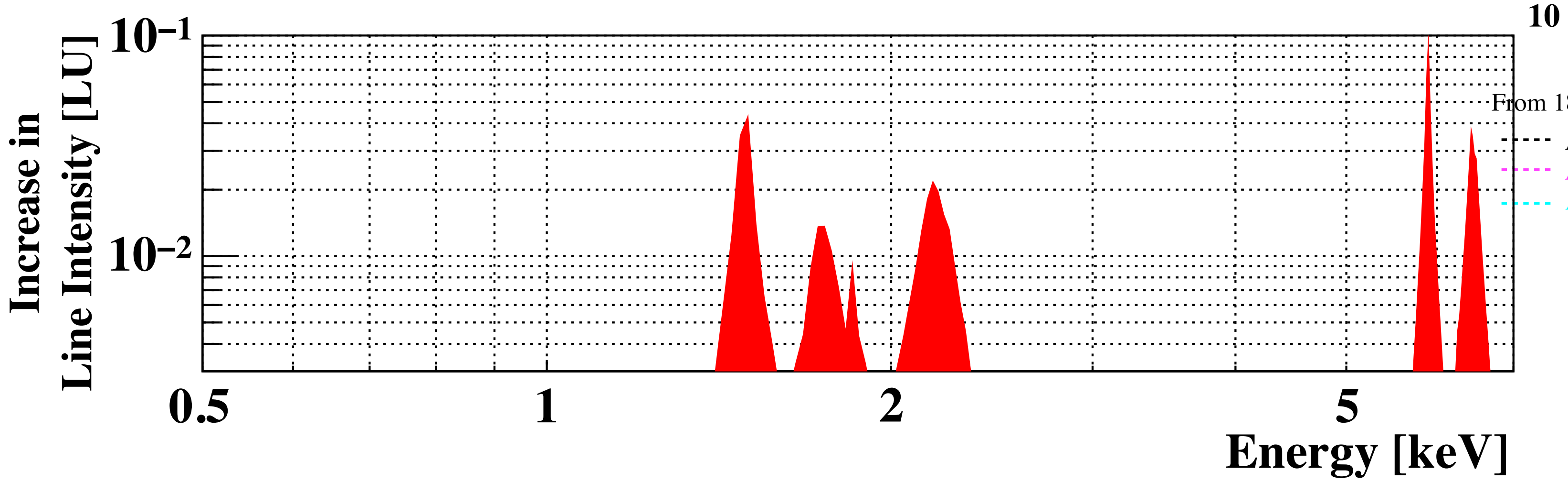

Look-Elsewhere Effect correction

As we do not know the "true" energy of DM,
we tried (7-0.5 keV)/25 eV = 260 lines.
a "3σ" line is expected ~ 260 * 0.0027 = 0.7
⇒ Look Elsewhere Effect (LEE) (see ex. Gross & Vitells, 2010)

We simulated 4000 mock spectra with the same response, emission and background models, and search "DM" lines to investigate false detection probability.

4.2 σ line: 5/4000⇒ p-value of 0.135 % or "3 σ"

3.2 σ line: 640/4000⇒ p-value of 15.9 % or "1 σ"

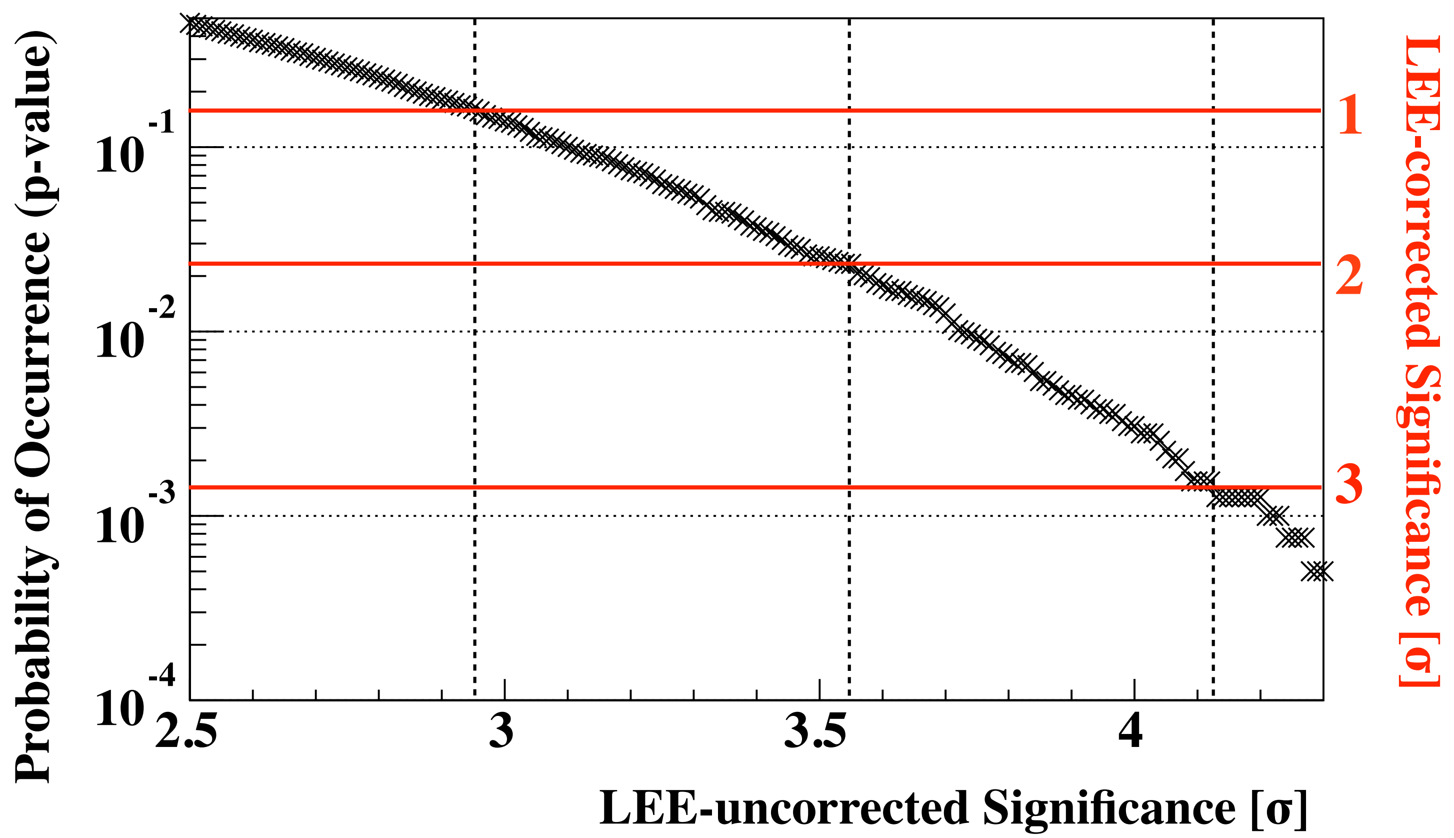

0.600 keV	~~2.8σ~~
0.900 keV	~~2.2σ~~
1.275 keV	~~2.4σ~~
4.925 keV	~~2.8σ~~
5.475 keV	~~2.4σ~~

All lines have confidence level of less than 1σ

Constraints on unknown emission line

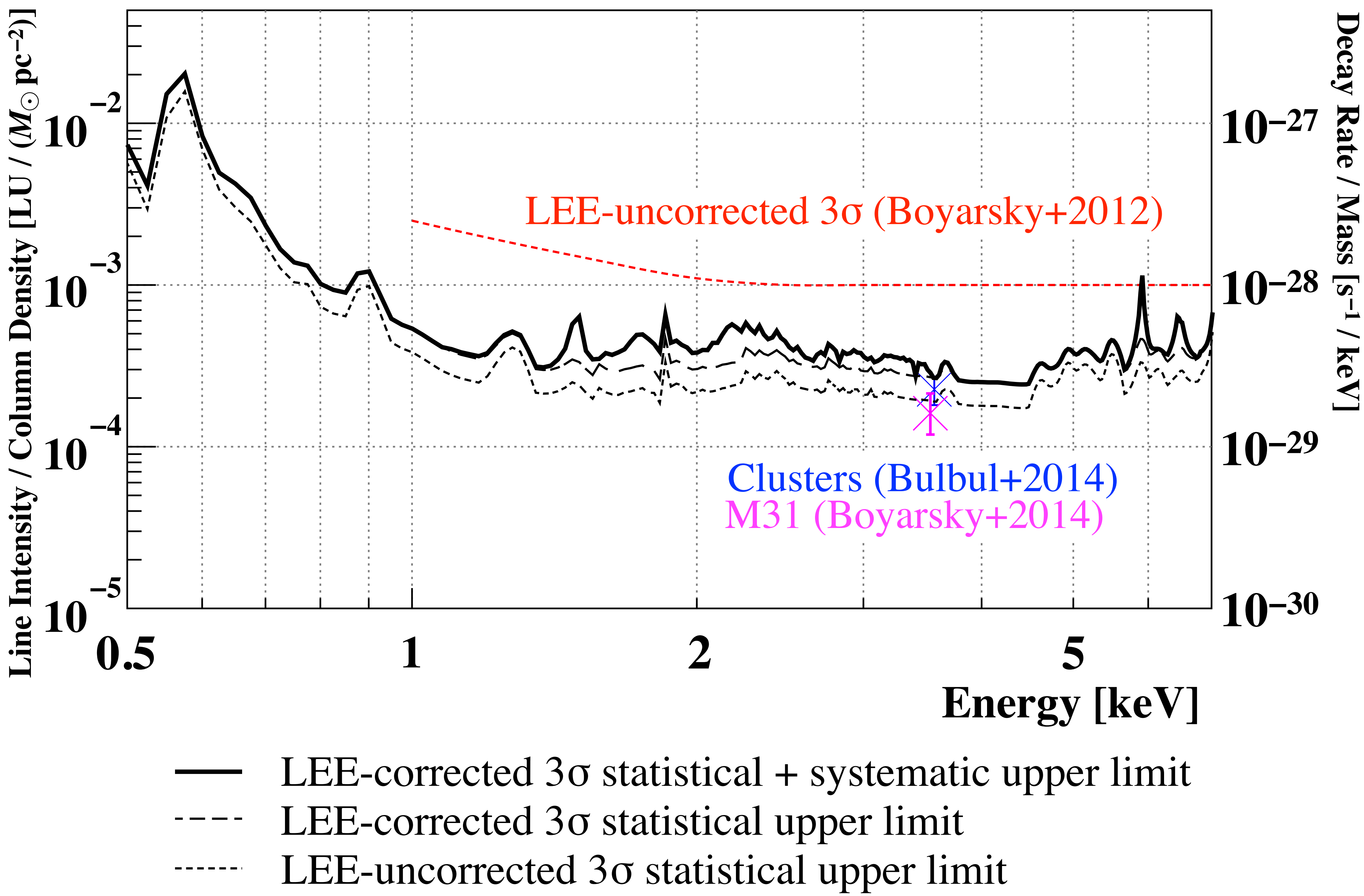

3σ=Max(Fit of 31.5Ms data, distribution of 4000 simulation)

Constraints on sterile neutrino mass and mixing angle

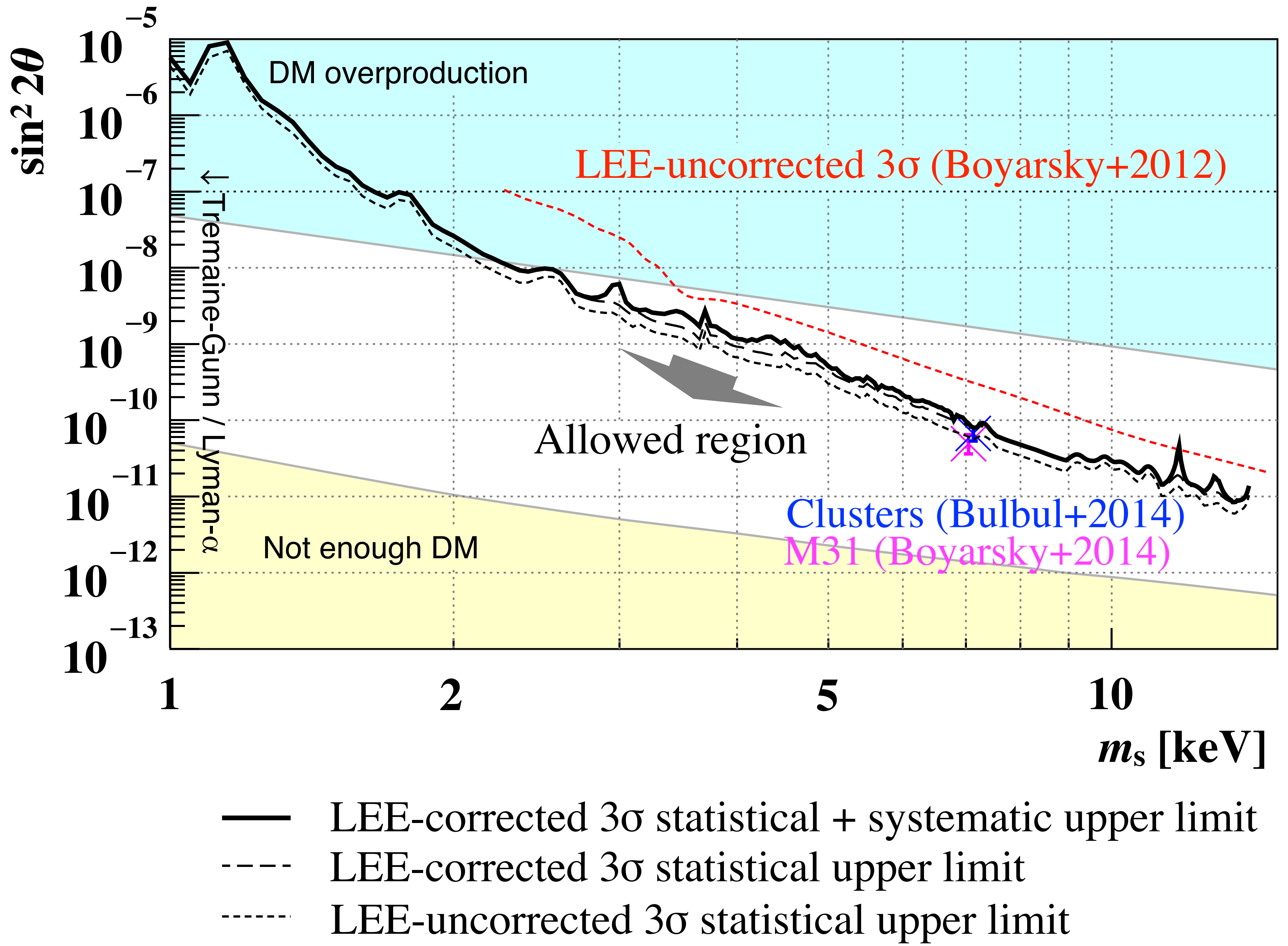

$$\Gamma = \frac{9\alpha {G_F}^2}{1024\pi^2} {m_s}^5 \sin^2 2\theta$$
$$= 1.4 \times 10^{-32} \left(\frac{m_s}{1\ \mathrm{keV}}\right)^5 \left(\frac{\sin^2 2\theta}{10^{-10}}\right) \ \mathrm{s}^{-1}$$

$$\Rightarrow I = 1.3 \times 10^{-5} \left(\frac{m_s}{1\ \mathrm{keV}}\right)^4 \left(\frac{\sin^2 2\theta}{10^{-10}}\right) \left(\frac{f_s}{1}\right) \left(\frac{S_{DM}}{10^2 M_\odot \mathrm{pc}^{-2}}\right) \ \mathrm{photons\ cm^{-2}\ s^{-1}\ sr^{-1}}$$

Future Prospects

Future prospects with Astro-H

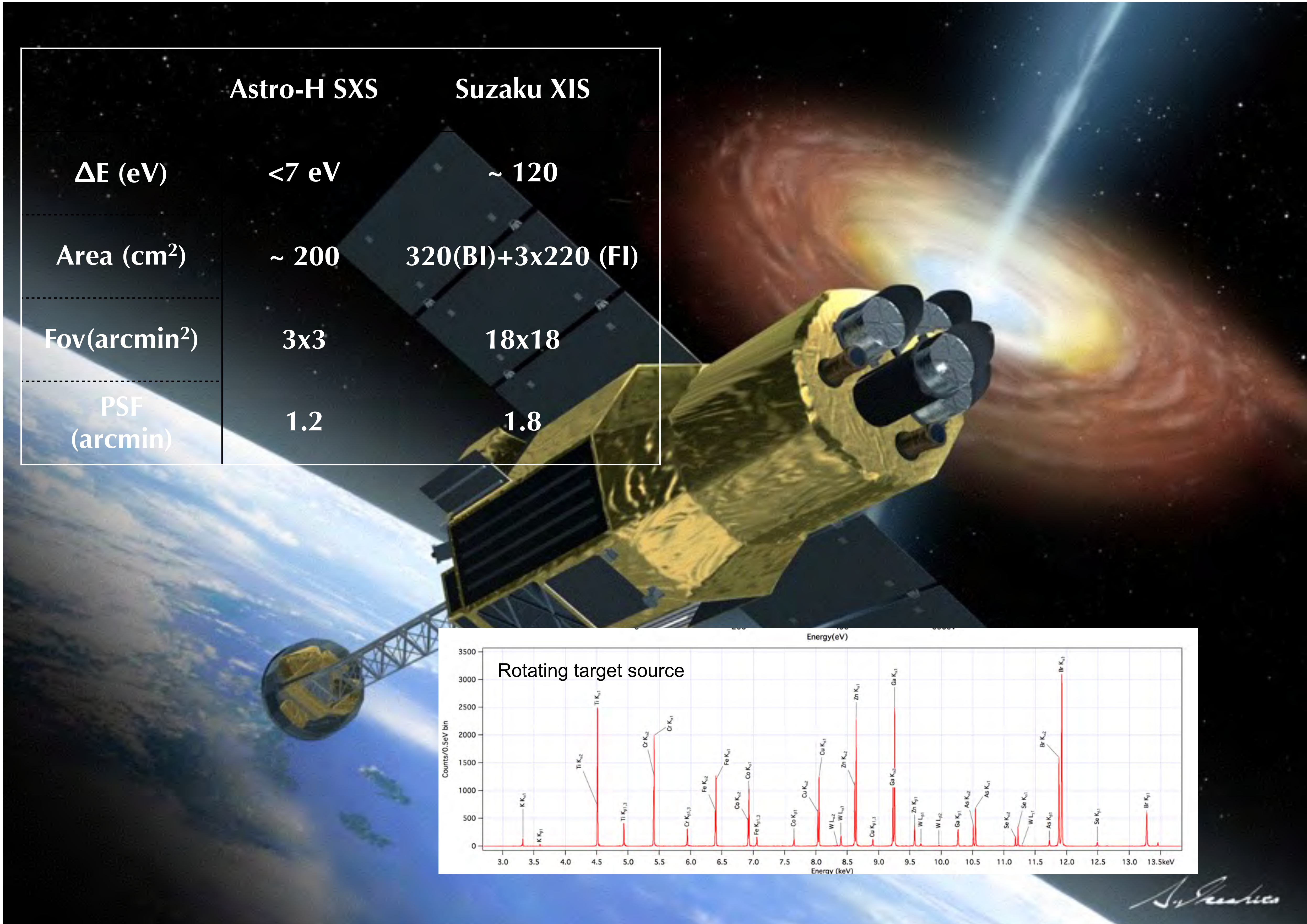

	Astro-H SXS	Suzaku XIS
ΔE (eV)	<7 eV	~ 120
Area (cm^2)	~ 200	320(BI)+3x220 (FI)
Fov($arcmin^2$)	3x3	18x18
PSF (arcmin)	1.2	1.8

SXS case study

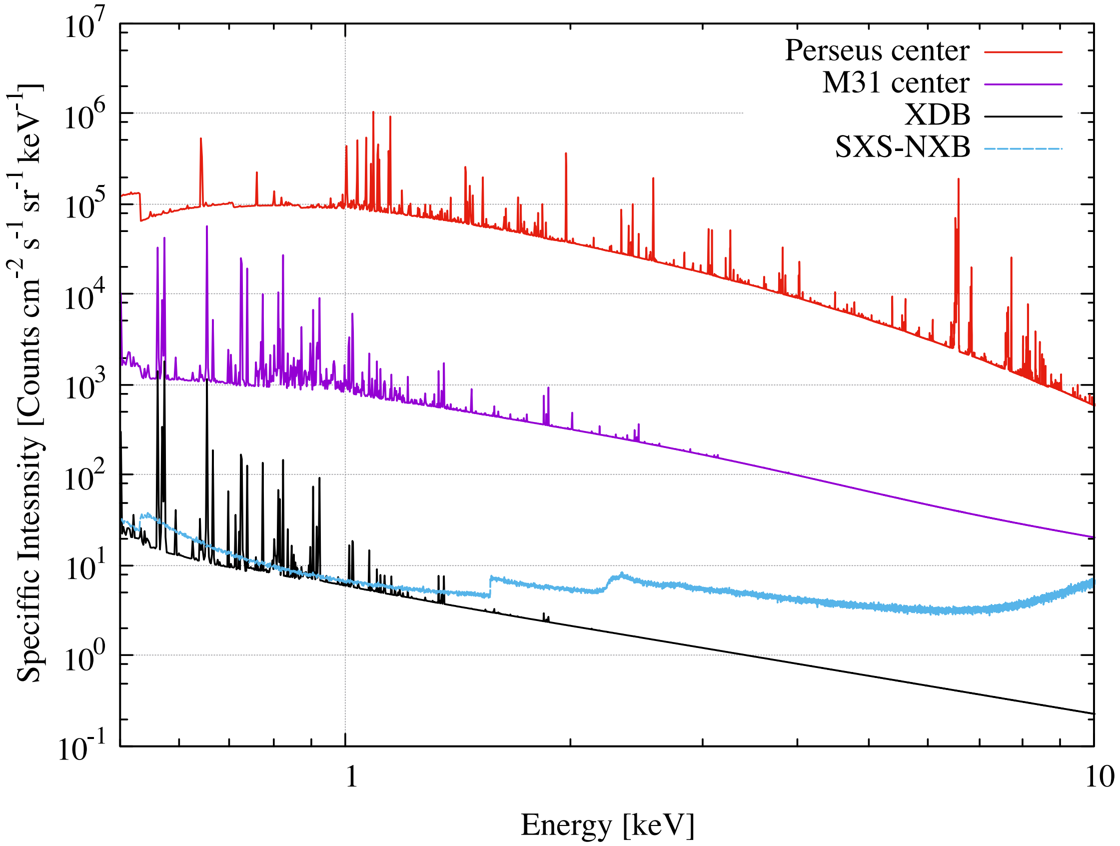

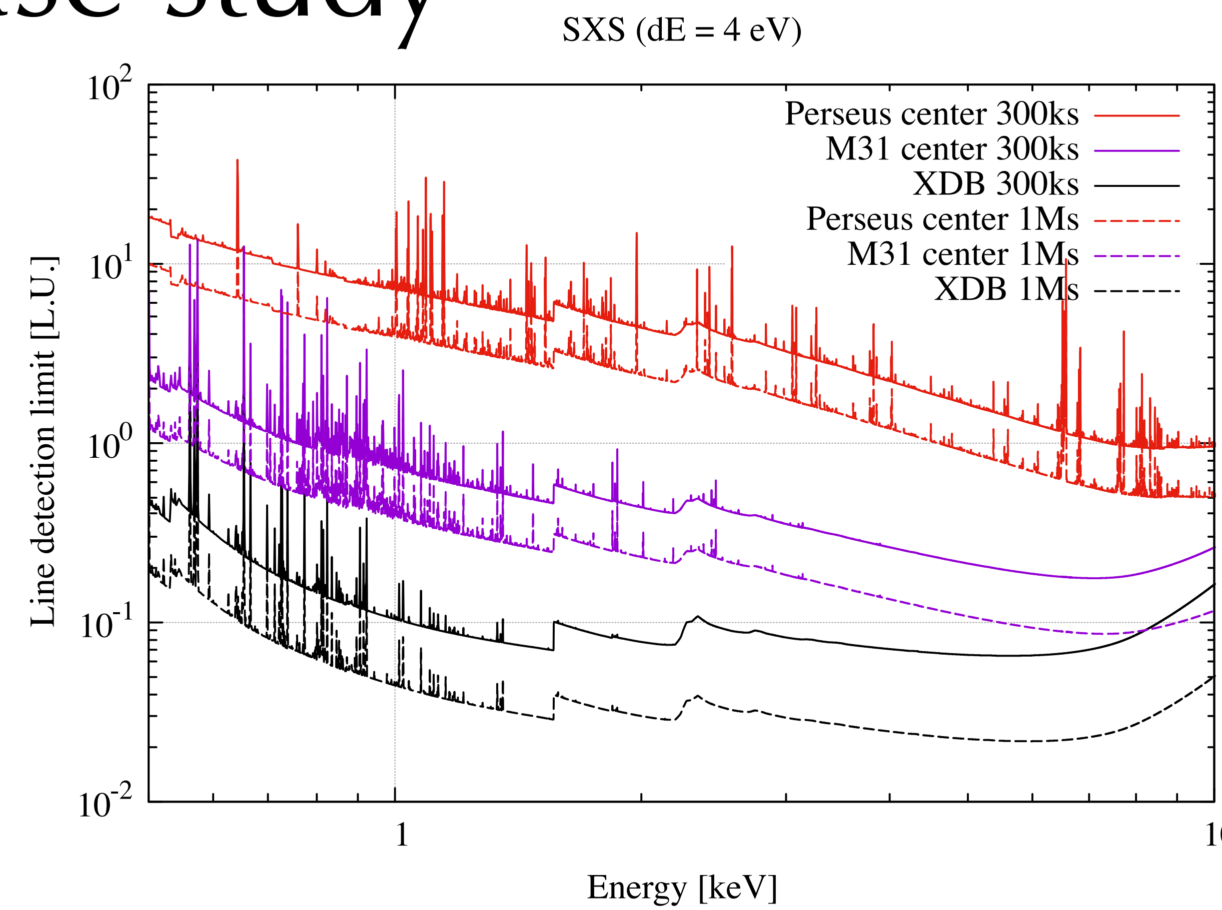

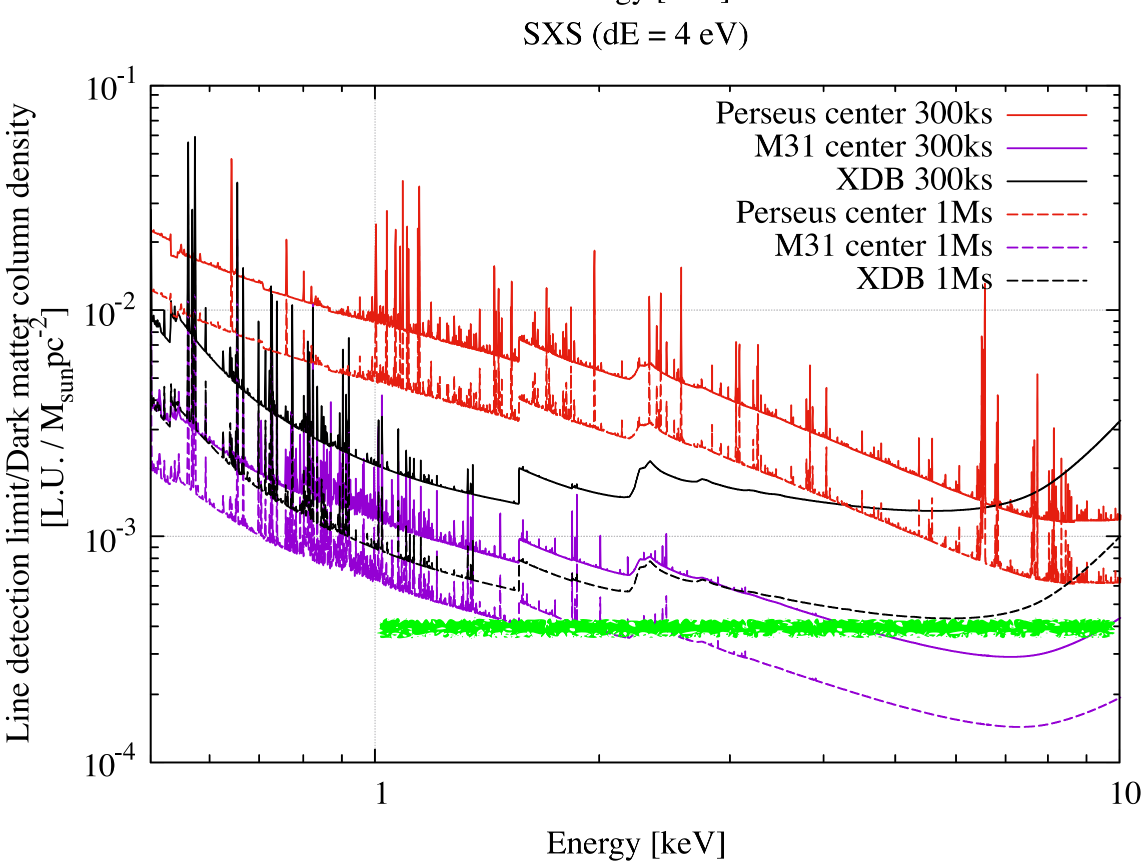

SXS: FOV is small, and blank sky data with large exposure time will not feasible.

M31 will be the best target.

~3σ of this study (Suzaku)

Summary and Conclusion

- ✓ To search X-ray signature from DM, we select the archival data of the soft X-ray background by Suzaku, as the current best method.
- ✓ In total 187 Suzaku observation with 31.5 Msec exposure between 2005 and 2013 are analyzed.
- ✓ We set the upper limits for keV-region DM with very careful study and LEE correction.
- ✓ It is possible to search deeply above 2 keV with M31 observation by Astro-H in future (but coming soon !)

See Tamura et al. PASJ, 67, 23 (2015) (arXiv:1412.1869)
& Sekiya et al. (arXiv:1504.02826)